Response to the Referees' Comments

First of all, we would like to give our sincerest thanks to the reviewers for the beneficial suggestions and comments, and we deeply appreciate your contributions, which help us for correcting and improving the manuscript. Our responses are listed as follows by using the red fonts. If there are still unclear or incorrect parts, the authors are very willing to make further corrections and improvements based on the reviewer's comments. Thanks again for your contributions.

Comment on "A multilayer approach and its application in modeling QGNSea V1.0: a local gravmetric quasi-geoid model over the North Sea" by Yihao Wu et al.
Anonymous Referee #3
Authors used the multilayer approach to model QGNSea V1.0 based on SRBF from the local terrestrial and ship-borne gravimetric data in the manuscript. The English writing should be further improved. The results may be of geodetic science sense by comparing with the local gravity data, GPS/leveling data, and the Earth gravity field models.

Response: The authors thank the reviewer for these beneficial comments. Based on the reviewer's comments, the authors have asked a native speaker to make a thorough language check of this manuscript, and we corrected all the grammar errors and bad language usages to improve its English level, please refer to the revised manuscript.

[1] Section 2.1 Study area and data. Here the local terrestrial and ship-borne gravity data are used in the study. Why not use the airborne gravity data and the satellite altimeter data? These data ever were used in Wu et al. 2017. Dr Wu is the first author in the manuscript. The results in the manuscript may be worse than those in Wu et al. 2017. More data can help to improve the resolution and the precision of QGNSea model. How to unify the datum of all data in the study?

Response: The authors thank the reviewer for these beneficial comments. Yes, we think the reviewer is right that the incorporation of more data help improve the resolution and the precision of QGNSea model. The solutions modeled in this study are inconsistent with ones shown in Wu et al. (2017c), since the input data and study area are different in these two studies. Yes, the solution modeled in this study may show worse results than the one displayed in Wu et al. (2017c), e.g., see the validation results in Belgium and Germany. The reasons are twofold. First, in this study we only use terrestrial and shipboard gravity data, no airborne or radar altimetry data are incorporated. While, for the solution A (without GOCE data) in Wu et al. (2017c), we used terrestrial, shipboard, and airborne gravity data, and radar altimetry data. Second, the target area in this study and the one in Wu et al. (2017b) are not consistent. The area in the study of Wu et al. (2017c) extends from 49.5 °N to 56 °N latitude and 0.25 °E to 8.25 °E longitude (see page 6 in Wu et al., 2017c); While, in this study we

choose a much larger area, which covers an area of 49 ℃N-61 ℃N latitude and -6 ℃E-10 ℃E (see page 3 in the original manuscript). And, when we choose a larger region, more data in UK, Norway, and the North Sea are incorporated. However, we notice that the data in Norway are sparse, especially in the mountainous regions, and this situation also occurs in the north parts of the North Sea, see Fig.2 in Wu et al. (2017c). Consequently, the quality of the solution may be affected if different gravity data are introduced, even when we validate the solution only use the GPS/leveling data in the Netherlands, Belgium, and Germany.

The motivation of this study is to develop a new parameterization of SRBFs network in the framework of the MRR idea, i.e., the so-called multilayer approach, and compare it with the traditionally-used single-layer approach for the performances in regional gravity field recovery. For a case study, we only use the terrestrial and shipboard gravity data, and the derived results show reasonable solutions, which can be used for supporting the conclusions of this study. For the time beings, the authors put effects on deriving reasonable solutions by combining heterogeneous gravimetry and altimetry data as well as GOCE data through the multilayer approach, and compare these solutions with ones modeled from the single-layer approach. However, more open issues need to be investigated since GOCE data mainly contribute to low-frequency bands of gravity field, and deeper layers than ones we use to combine surface data may be implemented to incorporate these satellite observations. The initial solutions seem to be promising, hopefully, we can obtain reasonable results, and make a detailed discussion regarding these issues in another paper. According to the reviewer's comments, we introduce this information in the conclusion part, see pp 32-33 in the revised version.

Yes, we need to unify the horizontal and vertical datums for all the gravity data, since these data were derived from various institutions over different time spans (see Wu et al. (2017c)). The European Terrestrial Reference System 1989 (ETRS89) and European Vertical Reference Frame 2007 (EVRF2007) are chosen as the horizontal and vertical systems (Slobbe, 2013), respectively. For terrestrial data in all regions except for the UK, transformation parameters can be directly used to unify the national vertical systems to EVRF2007. For shipborne data, the reference models derived from DTU13, i.e., mean sea surface (MSS) and mean dynamic topography (MDT), are used to extract the ellipsoidal and orthometric/normal height information. With respect to terrestrial data in the UK, the effects of the systematic errors are in its leveling system, where both the south-north slope and regional distortions exist, and no valid transformation parameters can be used for vertical datum unification (Penna et al., 2013). However, as EGM2008 has no slope when compared with the local corrected mean sea level values (Penna et al., 2013), we use it as the reference model for data reduction. Details can be found in Wu et al. (2017c). According to the reviewer's comments, we add the brief information for horizontal and vertical datums unification in the revised version, please see pp 4.

[2] Section 3 Numerical results and discussion. The full flow chart to build QGNSea model should be shown in detail, which can make readers to understand the technological idea in general.

Response: Thanks the reviewer for the comments. Yes, it is a very nice suggestion to build a full flow chart for model development based on the multilayer approach, which is pretty beneficial for potential readers. According to the reviewer's comment, we provide a detailed flowchart of designing the multilayer model, see Figure 1 in pp 11 in the revised manuscript. Also, a brief description is added, see pp 10 in the updated version.

[3] Section 3.1. What algorithm can be used to estimate automatically the order of wavelet analysis? What criterion can be used to judge the optimal order?

Response: The authors thank the reviewer for these beneficial comments. This is a very good question regarding the determination of optimal decomposition order. The authors believe it is still an open issue regarding the automatic determination of the optimal order for wavelet analysis. Usually, we preselect an order for wavelet decomposition, and this order is arbitrarily chosen to some extent. Then, we need to analyze the decomposed wavelet details and approximation for determining the optimal order. If there are still details that are needed for constructing the multilayer model haven't been separated, we need to change the decomposition order until all the useful details have been extracted; otherwise, we truncate to a specific order, and compute the wavelet details and approximation to construct the multiply layer's parameterization. Please see the details in Section 3.1 about how to choose the decomposition order in the case of this study. Since the analysis of the wavelet signals need the background knowledge of the local gravity field signals (i.e., the spectral contents of residual gravity signals), also human interventions are necessary for key parameters estimation and crucial choices during these procedures (e.g., the types of basis functions for wavelet decomposition and number of layers), thus it is difficult for make these procedures totally automatic. The future work may involve in developing a data-adaptive algorithm, however, additional efforts are needed. According to the reviewer's comment, we enhance this information in the conclusion part, please see pp 32 in the revised manuscript.

[4] Figure 1. What geological structure and geophysical mechanism are corresponding to each layer?

Response: Thanks the reviewer for these comments. Gravity anomaly primarily reflects the density heterogeneity of anomalous mass in the Earth interior. Density distributions at different depths are strongly correlated with the geological structure. Therefore, the decomposed gravity anomalies in the Figure 2 (Figure 1 in the original version) can reveal the tectonic structure of study area at various depths.

The source depths of D1 and D2 in Figure 2 are less than 3 km. They highly correlate with the local topography, mainly due to the uncorrected topographical signals. The anomalies in the ocean are smooth, while those on land are more dispersed. D3 and D4 with the respective source depths of 4.5 km and 9.2 km are corresponding to the tectonic structure in the upper crust. The Viking Graben located in the northern of the North Sea is in agreement with the dispersed gravity anomalies, while two basins (i.e. Forth Approaches Basin and Norwegian-Danish Basin) located in the south is in accordance with relatively smooth anomalies. The apparent positive-negative alternating patterns of D5 and D6 with the source depth of 13.7 km and 19.6 km are consistent with the crustal shearing and extrusion in the middle crust. D7 with the mean source depth of 27.0 km primarily reflects the Moho undulation. The D8 and A8 are smooth, corresponding to density distribution of the upper mantle. The detailed discussions are seen in Section 3.1 and 3.2 of the manuscript.

The motivation of this study is to develop a new parameterization of gravity field based SRBFs in the framework of MRR, and the wavelet decomposition and wavelet analysis are only used to separate the contributions of different anomaly sources, which are finally used to design the parameterizations of multiply layers. And, the detailed investigation of geological structure and geophysical mechanism in this area is out the scope of this study. The authors expect to make a detailed investigation of geological structure through the wavelet-based method based on gravity data over the North Sea, and compare it with the results derived from other data sources (e.g., GPS data and seismic wave data), and the raw manuscript is in preparation.

[5] Table 3. Please show the detailed algorithm and method to determine reasonably the depth of each layer.

Response: The authors thank the reviewer for this beneficial comment. The detailed algorithm and method to determine reasonably the depth of each layer can be referred to Spector & Grant (1970) and Xu et al. (2018). In the manuscript, we only show the primary equations (see Eq. (4) and Eq. (5)). The method is also presented in details as follows.

According to the solution to two-dimensional Lapalace's equation, each $D_w(\varphi,\lambda)$ of the eq. (4) in the manuscript can be expressed as (Spector and Grant, 1970; Syberg, 1972; Cianciara and Marcak, 1976):

$$D_w(\varphi,\lambda)=\sum_{\varphi}\sum_{\lambda}G_K e^{i2\pi(K_\varphi\varphi+K_\lambda\lambda)}e^{2\pi KH}$$

where G_K denotes the amplitude, $K=\sqrt{K_\varphi{}^2+K_\lambda{}^2}$ is the wave number, (φ,λ) is the geodetic latitude and longitude, and H is the elevation of $D_w(\varphi,\lambda)$. Thus, G_K can be determined by:

$$G_K = \sum_{\varphi}\sum_{\lambda} D_w(\varphi,\lambda) e^{-i2\pi(K_\varphi \varphi + K_\lambda \lambda)} e^{\pm 2\pi K H}$$

When $H = 0$, the last equation can be written as:

$$(G_K)_0 = \sum_{\varphi}\sum_{\lambda} D_w(\varphi,\lambda) e^{-i2\pi(K_\varphi \varphi + K_\lambda \lambda)}$$

Inserting this equation into G_K

$$G_K = (G_K)_0 e^{\pm 2\pi K H}$$

Hence,

$$P_K = (P_K)_0 e^{\pm 4\pi K H}$$

where $P_K = (G_K)^2$ is the power. Then,

$$\ln P_K = \ln(P_K)_0 \pm 4\pi K H$$

in which $\ln P_K$ is natural logarithm of P_K. Based on the linear correlation between K and $\ln P_K$, the corresponding average source depth h_w of $D_w(\varphi,\lambda)$ can be estimated as (Spector and Grant, 1970; Xu et al., 2018)

$$h_w = \frac{1}{4\pi}\frac{\Delta \ln P_K^w}{\Delta K_w} \quad w = 1, 2, \cdots, W$$

$\Delta \ln P_K^w$ and ΔK_w are the change rates for $\ln P_K^w$ and radial wave number K_w, respectively. In this manner, the corresponding average source depths h_w of all decomposed wavelet details $D_w(\varphi,\lambda)\ (w = 1, 2, \cdots, W)$ and wavelet approximation $A_W(\varphi,\lambda)$ can be computed.

According to the reviewer's comment, we add the detailed algorithm and method to determine reasonably the depth of each layer, please see pp 7-8 in the revised manuscript.

[6] Section 3.3. We all know that the precision of terrestrial gravity data is better than that of ship-borne gravity data. But 1.45 mGal is for the terrestrial gravity data and

1.30 mGal for the ship-borne gravity data. Why?

Response: We thank the reviewer's for the beneficial comments. Yes, for the raw gravity observations, terrestrial data usually have better qualities than shipboard measurements. The estimated posterior variance factor of terrestrial data (1.45 mGal) is larger than that of shipboard data (1.30 mGal), we believe it is mainly due to the more significant uncorrected terrain effects in land than in ocean. We model the local gravity field based on the remove-compute-restore (RCR) method, and only the residual gravity field is parameterized through the SRBFs based on the single-layer or multilayer approach. Thus, the residual gravity data (after removing the GGM-derived components and RTM corrections) rather than the original data are used for modeling. Due to the limited spatial resolution of gravity measurements, we use the RTM to recover the local high-frequency signals that cannot be extracted from the gravimetry measurements. We see the local gravity field becomes smooth on land with RTM corrections, especially in areas with topography variation, however, uncorrected signals remain, e.g., see the red signals around Fraserburgh in England (around -2 ℃W and 57.5 ℃N) and blue ones along the boundary between France and Germany (around 8 ℃W and 49 ℃N) (see Figure 2 and Section 3.2 in Wu et al. (2017c)), which are mainly due to the limitations of the DTM (in terms of both spatial resolution and precision) and inaccuracy of the density parameter for the topography. These uncorrected high-frequency errors inevitably propagate into the regional solutions when modeling with single-layer/multilayer approach, see the data residuals showing in Figure 6 (Figure 5 in the original version); and the most significant residuals concentrate at these mountainous regions where the data are relatively sparse and uncorrected terrain corrections remains. On the other hand, the marine gravity field seems to be less affected by the local topographical effects, mainly due to the relatively small variation of local bathymetry (see Section 3.2 in Wu et al. (2017c)), and less significant residuals show in ocean parts, see Figure 6. The posterior variance factors are directly computed based on the data residuals, e.g., see eq.(25) in Klees et al. (2008), thus the estimated value for terrestrial observation group demonstrates lower accuracy.

[7] Figure 5. How to reduce effectively the edge effects for the local model?

Response: The authors thank the reviewer for the comment. The boundary limits for the area of Figure 5 are contracted by 0.5 ° in all the directions to reduce the edge effects. According to the reviewer's comment, we add this information (see pp 20) and redraw the data residuals only inside the boundary limits of this area, see Figure 6 in the updated version. Also, the corresponding statistics for data residuals are changed, see pp 20 and Table 5 in pp 25.

[8] Table 5. Why all means are 0 in the table?

Response: The authors thank the reviewer for this comment. We believe the mean values for the residuals should be zero, the local gravity field is modeled in the

framework of least squares system, both for the single-layer and multilayer approach. As a result, the sum of the residuals after least squares adjustment is zero, and the mean values for different observation groups derived from different approaches should be zero.

[9] Page 22. The degree for EGM2008 is up to 2190, but the order for EGM2008 is not up to 2190.

Response: The authors thank the reviewer for this beneficial comment. Yes, we believe the reviewer is right, the full order of EGM2008 is 2159 not 2190. According to the reviewer's comment, we correct this information, please see pp 26 in the updated version.

[10] Figures 7 and 8, Table 7. Why remove the mean differences?

Response: Thanks the reviewer for the comments. Due to the commission errors and uncorrected systematic errors in gravity data and inconsistencies among different height datums, the various GGMs (e.g., EGM2008 and EIGEN-6C4) deviate from local values observed from GPS/leveling data by tens of centimeters levels or even larger in the area of this study. While, the local gravity field model like QGNSea seems suffers less from this problem (see the mean values in Table 6), mainly due to the incorporation of more high-quality data and refined data preprocessing procedures. Thus, if we don't remove the mean differences between the GGMs and local GPS/leveling data, these differences are almost dominated by these systematic biases, which is undesirable for model comparisons. After removing these biases, the accuracies of different models can be clearly shown in Figure 9 (Figure 8 in the original version) and Table 7, and we also remove the mean values of the differences between QGNSea and other models to make these comparisons consistent, see Figure 8 (Figure 7 in the original version). According to the reviewer's comment, we add this information to the revised version, please see pp 27 in the updated version.

[11] Figure 8. We can see the systematical differences in the figure. Why?

Response: Thanks the reviewer for this comment. Yes, we agree with the reviewer's comment that the systematic errors remain. The regional gravimetric model usually deviates from the local GPS/leveling data, mainly due to commission errors in the GGMs and uncorrected systematic errors in the data and height systems. The systematic errors still exist in the results shown in Figure 9 (Figure 8 in the original version), since these errors cannot be thoroughly by simply removing the mean differences. As shown in pp 23-24, several methods can be used for reducing these systematic errors, and properly combine GPS/leveling data and gravimetric solution. However, the target for this study is to develop a multilayer approach for gravimetric

quasi-geoid modeling, which is served as a basic surface for further geophysical applications. While, after implementing these methods for combining local GPS/leveling and gravimetric model, the derived quasi-geoid is not purely gravimetric. Besides, the final solution may be distorted if only the locally distributed GPS/leveling data are combined, especially in the ocean parts, since no control data exist in these regions, see the detailed discussion in pp 23-24. Similar results for comparing the GPS/leveling data and gravimetric solutions can be found in Wu et al. (2017a, c). According to the reviewer's comment, we add this information in the revised manuscript, please see pp 27 in the updated version.

A multilayer approach and its application ~~in modelingto QGNSea V1.0~~ model~~,~~: a local ~~gravmetric~~gravimetric quasi-geoid model ~~,~~over the North Sea: QGNSea V1.0

Yihao Wu[1, 2], **Zhicai Luo** [3], **Bo Zhong**[4], **Chuang Xu**[2, 5]

[1] School of Earth Sciences and Engineering, Hohai University, Nanjing, China

[2] State Key Laboratory of Geodesy and Earth's Dynamics, Institute of Geodesy and Geophysics, Chinese Academy of Sciences, Wuhan, China

[3] MOE Key Laboratory of Fundamental Physical Quantities Measurement, School of Physics, Huazhong University of Science and Technology, Wuhan, China

[4]School of Geodesy and Geomatics, Wuhan University, Wuhan, China

[5]School of Civil and Transportation Engineering, Guangdong University of Technology, Guangdong, China

Correspondence to: Yihao Wu (yihaowu@hust.edu.cn) and Chuang Xu (chuangxu@hust.edu.cn)

Abstract: A multilayer approach is set up for local gravity field recovery within the framework of multi-resolution representation, where the gravity field is parameterized as the superposition of ~~the multiply~~ multiple layers of Poisson wavelets located at ~~the~~ different depths beneath the Earth's surface~~topography~~. ~~Different~~ The layers are designed to recover ~~the gravitational~~gravity signals ~~at from the various levels,~~at different scales, where the shallow and deep layers ~~each~~ mainly capture the short- and long-wavelength signals, respectively. The depths of these layers ~~beneath the topography~~ are linked to the locations of ~~that~~ different anomaly sources beneath the Earth's surface ~~locate~~, which ~~were~~are estimated by ~~the~~ wavelet decomposition and power spectrum analysis. For testing the performance of this approach, a gravimetric quasi-geoid model over the North Sea, QGNSea V1.0, ~~was~~is ~~applied to the region over the North Sea, in Europe called QGNSea V1.0 is computed and~~This model was also ~~compared with other existing models~~modeled and validated against independent control data. The results show that the multilayer approach fits the gravity data better than the traditional~~ly used~~ single-layer ~~one~~approach, ~~especially~~ particularly in regions with topographical variation. An Akaike information criterion (AIC) test ~~demonstrates~~ showeds that the multilayer model ~~gives~~ obtains a smaller AIC value and~~,~~ ~~reaches~~ achieves a better balance between the goodness of fit of data and the simplicity of the model. ~~Moreover~~Further, an ~~the~~ evaluation ~~with~~ using independent GPS/leveling data ~~that~~ tests the ability of regional models computed from different approaches ~~of~~ towards realistic extrapolation~~, of regional models computed from different approaches~~ which ~~, showing~~ showeds that the accuracies of the QGNSea V1.0 ~~modeled from~~

~~using~~derived from the multilayer approach are ~~improved~~ better by 0.4 cm, 0.9 cm, and 1.1 cm in the Netherlands, Belgium, and parts of Germany, respectively, ~~compared to the solution~~than that ~~computed from~~using the single-layer approach. Further validation with existing models shows that QGNSea V1.0 ~~has the best quality~~is superior with respect to performance and~~,~~ ~~which~~ may be beneficial for studying ~~the~~ ocean circulation between the North Sea and its neighbo~~u~~ring waters.

1. Introduction

Know**ledge~~ing~~** of the earth's gravity field at the regional scale~~s~~ is crucial for a variety of applications in geodesy. It not only facilitates the use of the Global Satellite Navigation System to determine orthometric/normal heights in geodesy and surveying engineering, but also plays a fundamental role ~~in~~ in oceanography and geophysics.

Regional gravity field determination is typically ~~implemented~~ conducted within ~~a~~ the framework of the remove-compute-restore methodology (RCR) (Sjöberg, 2005), where ~~the~~ long-wavelength signals are often recovered by satellite-only global geopotential models (GGMs) derived from ~~the~~ dedicated satellite gravity missions~~,~~ such as the GRACE (Gravity Field and Climate Experiment) (Tapley et al., 2004) and GOCE (Gravity Field and Steady-State Ocean Circulation Explorer) (Rummel et al., 2002). Middle- and short-wavelength signals are extracted from ~~the~~ locally distributed gravity-related measurements (Guo et al., 2010; Wang et al., 2012; Wang et al., 2018). Spherical radial basis functions (SRBFs) ~~are~~ have become of great interest for gravity field modeling at the regional scale~~s~~ in the recent~~over~~ years (Eicker et al., 2013; Naeimi et al., 2015). Typically, the ~~widely used~~most commonly SRBFs are~~method is~~ implemented ~~by~~ using the ~~the so-called~~ single-layer approach, ~~i.e.,~~i.e. ~~where~~ the parameterization of the gravity field is ~~only~~ based on only a single-layer of the SRBF~~s'~~ grid (Wittwer, 2009; Bentel et al., 2013; Slobbe, 2013; Wu et al., 2016a).

It has been suspected for long that ~~if~~ the single-layer approach ~~can~~ may fail to extract the full information ~~of~~ contains in local gravity data~~, in full,~~ ~~and~~ thus the multi-resolution representation (MRR) method with SRBFs has been investigated ~~over~~ in the recent years (Freeden et al., 1998; Fengler et al., 2004, 2007). Freeden and Schreiner (2006) proposed a multi-scale approach based on ~~the~~ locally supported wavelets for determining ~~the~~ regional geoid undulations from ~~the~~ deflections of the vertical. Further, Freeden et al. (2009) demonstrated that ~~the~~ a multi-scale approach using spherical wavelets provided a powerful technique for the investigation of, local fine-structured features

such as those caused by plumes, which allowed ~~a~~ the scale- and space-dependent characterization of this geophysical phenomenon. Schmidt et al. (2005, 2006, 2007) developed a multi-representational method for static and spatiotemporal gravitational field modeling ~~through~~ using SRBFs, where the input gravity signals were decomposed into a ~~certain~~ number of frequency-dependent detail signals~~;~~, ~~and~~ they concluded that this approach could improve the spanning fixed time intervals with respect to the usual time-variable gravity fields. Chambodut et al. (2005) set up a multi-scale method for magnetic and gravity field recovery using Poisson wavelets~~,~~ and created a set of hierarchical meshes associated with the wavelets at different scales, where a level of subdivision corresponded to a given wavelet scale. Panet et al. (2011) extended the approach developed by Chamboudt et al. (2005)~~,~~ ~~and~~ by ~~applied~~ applying a domain decomposition approach to ~~define~~ defining the hierarchical subdomains of wavelets at different scales~~;~~, ~~which allowed to~~this enabled the splitting of a large problem into smaller ones. The~~se~~ results of these studies show that the multi-scale approach ~~with~~ using SRBFs has a good ~~prospective in~~potential for gravity field recovery~~.~~, ~~however~~However, to the best of our knowledge, no direct comparisons have been made between the single-layer approach and the multi-scale one regarding their performances in local gravity field recovery. ~~Besides~~Further, the existing multi-scale methods mainly construct the multi-scale framework in a mathematical sense, ~~where~~ and no explicit geophysical meanings are investigated. In this study, inspired by the power spectral analysis of local gravity signals, we develop ~~a~~ new parameterizations of the SRBF~~s~~ network within the ~~framework of the~~ MRR ~~idea~~approach~~,~~ ~~i.e.,~~ ~~the so-called multilayer approach; and~~ In this approach, ~~the multiply~~ multiple layers are linked to the anomaly sources at different depths beneath the ~~topography~~Earth's surface, ~~which~~ and the aim ~~at~~ is to recover~~ing~~ the signals with different spectral contents.~~at different levels. In this way~~Thus, ~~the parameterization of in the multi-scale method can be linked~~is related to the different anomaly sources at the different depths.~~ Moreover, the performances of the multilayer approach and traditional~~ly used~~ single-layer ~~one~~ approach are directly compared ~~in this study~~, ~~where~~ and the advantages and disadvantages of ~~different~~ the two methods are analyzed.

The structure of the manuscript is as follows.~~:~~ T~~t~~he ~~data in a study area in Europe~~study area and data collection methods are ~~firstly~~ described in Section 2. Then, the ~~multilayer approach based on the~~ MRR ~~representation~~ method with SRBFs is introduced~~,~~ where Poisson wavelets that have band-limited properties are chosen as the basis functions. ~~and the w~~Wavelet decomposition and power spectrum analysis are applied ~~for~~ in constructing the network of ~~networks of~~ Poisson wavelet~~s networks s with the multilayer~~in this ~~approach~~. In addition, the function model based on ~~the~~ this multilayer approach is ~~set up~~derived~~,~~ and the method for estimating the unknown coefficients of Poisson wavelets is

introduced. ~~We~~ The construction of the multilayer model is described in S~~s~~ection 3.~~,~~ ~~and compare t~~The performances of ~~different~~ the two approaches ~~(traditional~~ single-layer and multi-layer) are also compared in this section. Finally, ~~the~~ a gravimetric quasi-geoid over the North Sea, called QGNSea V1.0, is modeled ~~by~~ using the multilayer approach and compared with other models for cross validation~~s~~. We ~~summarize~~ present the ~~main summaries~~ summary and the main conclusions of this study in S~~s~~ection 4.

2. Data and method~~s~~

2.1. Study area and data

A ~~local~~ region in Europe, from 49 °N to 61 °N and -6 °E to 10 °E, ~~–~~covering the mainland of the Netherlands, Belgium, parts of the North Sea, UK, Germany, and France is chosen as a case study~~, which covers an area of 49 °N-61 °N latitude and -6 °E-10 °E longitude., including the mainland of the Netherlands, Belgium, and parts of the North Sea, UK, Germany and France.~~ Data regarding p~~P~~oint-wise terrestrial and shipborne gravity anomalies ~~are were incorporated obtained for to testing the approach we developed~~are used in this study, which were provided by different institutions~~,~~ ~~see Slobbe et al. (2014)~~. The details ~~for~~ of the data pre-processing procedures can be ~~referred to~~found in Wu et al. (2017c), where crossover adjustment and low-pass filters were applied to remove systematic errors and reduce high-frequency noise, respectively. Since the terrestrial and shipborne gravity data ~~se data~~ were derived from ~~various~~ different institutions over ~~different~~ various time spans, ~~and~~ the horizontal and vertical datums need to be unified. The European Terrestrial Reference System 1989 (ETRS89) and European Vertical Reference Frame 2007 (EVRF2007) are chosen as the horizontal and vertical systems ~~(Slobbe, 2013)~~, respectively (Slobbe, 2013). ~~And, d~~Datum transformations ~~are~~ were performed on all of the data following the methods proposed by ~~, details can be found in~~ Wu et al. (2017c). Moreover, the long-wavelength signal content in the data is reduced by removing the contribution of the ~~satellite-only reference model called~~ GOCO05s global geopotential model complete to~~, with a full~~ degree and order (d/o) of 280 (Mayer-Gürr et al., 2015).~~,~~ At the very short wavelengths, ~~and~~residual terrain model (RTM) ~~RTM corrections were removed from the original observations to decrease the signal correlation length and smooth the data within the framework of remove-compute-restore (RCR) framework~~is applied. The details ~~for~~ of the RTM reduction process and the residual gravity data can be found in Wu et al. (2017c).

2.2. Multilayer approach

According to Schmidt et al. (2006, 2007), the ~~multi-resolution representation (~~MRR~~)~~ of the Earth's disturbing potential $T(\boldsymbol{z})$ ~~on~~ at position $\boldsymbol{z}$ is expressed as

$$T(\boldsymbol{z}) = \bar{T}(\boldsymbol{z}) + \sum_{i=1}^{I} t_i(\boldsymbol{z}) + \delta(\boldsymbol{z}) \tag{1}$$

where ~~$T(\boldsymbol{z})$ is the disturbing potential in this study,~~ $\bar{T}(\boldsymbol{z})$ ~~means~~ represents a reference model, ~~e.g.,~~e.g. a global geopotential model (GGM) computed from spherical harmonics; $\delta(\boldsymbol{z})$ represents ~~the~~ unmodeled signals; I is the number of levels (resolutions); $t_i(\boldsymbol{z})$ is the detailed signal of level i, and the higher the level value i is, the finer are the structures extractable from the input data; $t_i(\boldsymbol{z})$ is computed as ~~the~~ a linear combination of SRBFs (Schmidt et al., 2007).

$$t_i(\boldsymbol{z}) = \sum_{n=1}^{N_i} \beta_{i,n} \Psi_i(\boldsymbol{z}, \boldsymbol{y}_{i,n}) \tag{2}$$

where $\Psi(\boldsymbol{z}, \boldsymbol{y})$ is the SRBF, N_i and $\beta_{i,k}$ are the number and unknown coefficient of the SRBF at level i, respectively, and $\boldsymbol{y}_{i,n}$ is the position of the SRBF at this level.

~~We work with T~~the ~~RCR technique is used to remove, and t~~The reference GGM and RTM corrections are removed from the original data to decrease the signal correlation length and smooth the data (Omang and Forsberg, 2000). Then, only the residual ~~gravity gravitational~~disturbing potential $T_{res}(\boldsymbol{z})$ is parameterized by the SRBF~~s~~ using the MRR approach. ~~Neglecting~~ Ignoring the unmodeled signals, the residual disturbing potential is expressed as a series of ~~the~~ detailed signals at different levels~~, when~~ combining ~~E~~eq. (1) and e~~E~~q. (2)

$$T_{res}(\boldsymbol{z}) = \sum_{i=1}^{I} \sum_{n=1}^{N_i} \beta_{i,n} \Psi_i(\boldsymbol{z}, \boldsymbol{y}_{i,n}) \tag{3}$$

where Ψ_i is computed as the difference ~~of~~ between the spherical scaling functions with low-pass filter characteristics ~~between~~ corresponding to~~the~~ consecutive levels $i+1$ and i~~,~~; Ψ_i ~~but also~~ can also be expressed as the SRBF ~~has the~~with band-limited properties in the frequency domain (Schmidt et al., 2007). ~~In this study,~~ Ψ ~~is chosen as~~

~~the~~represents Poisson wavelets with band-limited properties (Chambodut et al., 2005) in this study, ~~and its~~the ~~full~~ complete definition of which can be found in Holschneider and Iglewska-Nowak (2007).

Poisson wavelets can also be identified as the multipoles inside the Earth, and the scales of Poisson wavelets can be linked to their depths beneath the Earth's surface.~~,~~ ~~which~~ These depths are the key parameters ~~issues that~~in determining~~e~~ ~~their~~ wavelet properties in space and frequency domains (Chambodut et al., 2005). The detailed signal at level i in e~~E~~q. (2) can be estimated ~~by~~ using a linear combination of Poisson wavelets located at a specific depth. Poisson wavelets at various depths demonstrate different properties in the frequency domain.~~,~~ At shallow depths, the scales decrease, and wavelet spectrums shift toward the high degrees of the spherical harmonics (SH) and become more sensitive to local signal features with high-frequency properties, and vice versa (Chambodut et al., 2005). Moreover, Poisson wavelets at different depths can be linked to the detailed signals at various levels, and are sensitive to the various spectral contents of input signals. They can be used for multi-resolution representation. ~~At shallowas the depths going shallower, the scales decrease, and wavelettheir spectrums shift towards the high degrees of the spherical harmonics (SH) and become more sensitive to the local signal features of signals with high-frequency properties, and vice versa (Chambodut et al., 2005).~~ These properties are crucial for local gravity field modeling. ~~First, t~~The residual disturbing potential is typically ~~the~~ a band-limited signal within the RCR framework, and Poisson wavelets with band-pass filter characteristics are preferable for band-limited signal recovery (Bentel et al., 2013). ~~Moreover, Poisson wavelets at different depths can be linked to the detailed signals at various levels, which are sensitive to different spectral contents of input signals, and can be used for multi-resolution representation.~~

Rather than ~~using the name of~~as an MRR, we interpret ~~Eq~~eq. (3) as the multilayer approach ~~considering~~that takes into consideration that Poisson wavelets at different depths have ~~various~~ different characteristics, and ~~the~~ different layers ~~are corresponding~~correspond to ~~the~~ Poisson wavelets' grids at various depths. We place the Poisson wavelets ~~on~~ in the Fibonacci grids under the Earth's ~~topography~~surface, and keep these grids parallel with the ~~topography~~ Earth's surface (Tenzer et al., 2012). Instead of associating the Poisson wavelets at different depths to the hierarchical meshes with various levels (Chambodut et al., 2005), we apply a wavelet analysis approach to estimate the depths of multiple~~y~~ layers.~~,~~ This approach is inspired by the power spectrum analysis of the local~~residual~~ gravity ~~field~~signals. ~~The power spectrum analysis of local gravity signals~~, which shows ~~the~~ that the gravity signals are ~~the~~ superpositions of ~~the contributions generated~~those~~contributions~~ from the anomaly sources at different depths,~~;~~ and the signals originating~~d~~

from different anomaly sources have heterogeneous spectral contents (Spector and Grant, 1970; Syberg, 1972; Xu et al., 2018). Since the Poisson wavelets at different depths are sensitive to signals with heterogeneous frequency characteristics, we ~~put~~ place Poisson wavelet~~s'~~ grids at ~~the~~ locations where ~~the~~ anomaly sources situate. In this manner, the contributions ~~from~~ of the anomaly sources at various depths can be estimated ~~by different layers~~.

In order to separate the contributions ~~stemmed from~~ of different anomaly sources, the wavelet multi-scale analysis~~, which is an excellent approach to extract the signals at different scales,~~ is applied to decompose the gravity data $\Delta g(\varphi,\lambda)$ into wavelet approximation $A_W(\varphi,\lambda)$ and a number of wavelet details $D_w(\varphi,\lambda)$ $(w=1,2,3,\cdots,W)$ at different scales (Jiang et al., 2012; Audet, 2013; Xu et al., 2017).

$$\Delta g(\varphi,\lambda)=A_W(\varphi,\lambda)+\sum_{w=1}^{W}D_w(\varphi,\lambda) \tag{4}$$

where (φ,λ) is the geodetic latitude and longitude, W is the maximum order for decomposition, $A_W(\varphi,\lambda)$ is the regional anomaly caused by deep and large-scale geological bodies, and $D_w(\varphi,\lambda)$ is the local anomaly originat~~ed~~ing from shallow and small-scale heterogeneous substances. Wavelet~~s~~ analysis generates low-order wavelet details that are ~~invariant with~~constant despite the decomposition order~~;~~, ~~and~~ only ~~the~~ high-order wavelet details and the corresponding wavelet approximation change with ~~the~~ decomposition order. Based on this ~~property~~, we can choose the proper decomposition order to ~~derive~~ obtain ~~the~~ desirable solutions.

According to the solution to the two-dimensional Lapalace's equation, each $D_w(\varphi,\lambda)$ in eq. (4) can be expressed as (Spector and Grant, 1970; Syberg, 1972; Cianciara and Marcak, 1976)

$$D_w(\varphi,\lambda)=\sum_{\varphi}\sum_{\lambda}G_K e^{i2\pi(K_\varphi\varphi+K_\lambda\lambda)}e^{2\pi KH} \tag{5}$$

where G_K denotes the amplitude, $K=\sqrt{K_\varphi{}^2+K_\lambda{}^2}$ is the wave number~~,~~, and ~~–~~ H is the elevation of $D_w(\varphi,\lambda)$. Thus, G_K can be determined ~~by:~~as:

$$G_K = \sum_{\varphi}\sum_{\lambda} D_w(\varphi,\lambda) e^{-i2\pi(K_\varphi \varphi + K_\lambda \lambda)} e^{\pm 2\pi K H} \tag{6}$$

When $H = 0$, eq. (6) can be written as

$$(G_K)_0 = \sum_{\varphi}\sum_{\lambda} D_w(\varphi,\lambda) e^{-i2\pi(K_\varphi \varphi + K_\lambda \lambda)} \tag{7}$$

Inserting eq. (7) into eq. (6), G_K is rewritten as

$$G_K = (G_K)_0 e^{\pm 2\pi K H} \tag{8}$$

Hence,

$$P_K = (P_K)_0 e^{\pm 4\pi K H} \tag{9}$$

where $P_K = (G_K)^2$ is the power. Then,

$$\ln P_K = \ln(P_K)_0 \pm 4\pi K H \tag{10}$$

~~in which~~where $\ln P_K$ is the natural logarithm of P_K. Based on the linear correlation between K and $\ln P_K$ in eq. (10), the corresponding average source depth, h_w, of $D_w(\varphi,\lambda)$ can be estimated as (Spector and Grant, 1970; Xu et al., 2018)

$$h_w = \frac{1}{4\pi}\frac{\Delta \ln P_K^w}{\Delta K_w} \quad w = 1, 2, \cdots, W \tag{11}$$

where $\Delta \ln P_K^w$ and ΔK_w are the change rates ~~for~~ of $\ln P_K^w$ and K_w, respectively. In this manner, the corresponding average source depths $h_w\ (w = 1, 2, \cdots, W)$ of all decomposed wavelet details $D_w(\varphi,\lambda)\ (w = 1, 2, \cdots, W)$ and wavelet approximation $A_W(\varphi,\lambda)$ can be estimated.

In this study, terrestrial and shipborne gravity anomalies are merged for modeling. Gravity anomalies, Δg, and

quasi-geoid heights, ζ, are related to the disturbing potential based on the multilayer approach as follows:

$$\begin{aligned}\Delta g(\boldsymbol{z}) &\approx -\frac{2}{|\boldsymbol{z}|}T_{res}(\boldsymbol{z})-\frac{\partial T_{res}(\boldsymbol{z})}{\partial|\boldsymbol{z}|}\\ &=\sum_{i=1}^{I}\sum_{n=1}^{N_i}\beta_{i,n}\left(-\frac{\partial}{\partial|\boldsymbol{z}|}\Psi_i(\boldsymbol{z},\boldsymbol{y}_{i,n})-\frac{2}{|\boldsymbol{z}|}\Psi_i(\boldsymbol{z},\boldsymbol{y}_{i,n})\right)\\ \zeta(\boldsymbol{z}) &= \frac{T_{res}(\boldsymbol{z})}{\gamma(\boldsymbol{z})}=\sum_{i=1}^{I}\sum_{n=1}^{N_i}\beta_{i,n}\frac{\Psi_i(\boldsymbol{z},\boldsymbol{y}_{i,n})}{\gamma(\boldsymbol{z})}\end{aligned} \tag{12}$$

where γ is the normal gravity value.

We ~~suppose~~ assume the observational errors ~~are~~ to be white noise~~s~~ with zero mean, and the gravity field model using the multilayer approach is ~~written~~ expressed as the standard Gauss-Markov model

$$\boldsymbol{l}_j-\boldsymbol{e}_j=\boldsymbol{A}_j\boldsymbol{x},\ E\{\boldsymbol{e}_j\}=0,\ \mathrm{D}\{\boldsymbol{e}_j\}=\boldsymbol{C}_j=\sigma_j^2\boldsymbol{Q}_j=\sigma_j^2\boldsymbol{P}_j^{-1},\quad j=1,2,\cdots,J \tag{13}$$

where $\boldsymbol{l}_j$ is the $m_j\times 1$ corresponding observation vector of group j, $\boldsymbol{e}_j$ is the $m_j\times 1$ vector of observational errors, $\boldsymbol{A}_j$ is the $m_j\times N$ design matrix of group j, $\boldsymbol{x}$ is the $N\times 1$ vector of unknown coefficients, including the unknown parameters of Poisson wavelets of all the layers, i.e. $\boldsymbol{x}=\left[\beta_{1,1},\beta_{1,2},\cdots,\beta_{1,N_1},\beta_{2,1},\beta_{2,2},\cdots,\beta_{2,N_2},\cdots,\beta_{I,1},\beta_{I,2},\cdots,\beta_{I,N_I}\right]'$, and $N=N_1+N_2+\cdots+N_I$; m_j is the number of observations in group j, and J is the number of observation groups. $E\{\cdot\}$ and $D\{\cdot\}$ are the expectation and dispersion operators, respectively. $\boldsymbol{C}_j$ is the error variance-covariance matrix of group j, and σ_j^2, $\boldsymbol{Q}_j$ and $\boldsymbol{P}_j$ are the variance factor, cofactor matrix, and weight matrix of group j, respectively.

The d~~D~~ata in different groups are assumed to be independent, and the weight matrix $\boldsymbol{P}_j$ is ~~supposed~~ assumed ~~to be~~as the scaled diagonal matrix with white noise properties since it is usually difficult to acquire ~~the~~ a realistic full error variance-covariance matrix in real-life measurements. Point-wise data can be directly combined for modeling through

the functionsal described above. However, the heterogeneous characteristics of the data, in terms of spatial coverages and noise properties, may result in an ill-conditioned normal matrix (Panet et al., 2011). We apply the first-order Tikhonov regularization for tackling the problem of the ill-conditioned matrix problem (Kusche and Klees, 2002; Wu et al., 2017a). For a given α (regularization parameter) and κ (regularization matrix), the least-squares solution of eq. (13) is (Klees et al., 2008):

$$\hat{\boldsymbol{x}} = \left(\sum_{j=1}^{J} \left(\frac{1}{\sigma_j^2} \boldsymbol{A}_j^T \boldsymbol{P}_j \boldsymbol{A}_j \right) + \alpha\kappa \right)^{-1} \left(\sum_{j=1}^{J} \left(\frac{1}{\sigma_j^2} \boldsymbol{A}_j^T \boldsymbol{P}_j \boldsymbol{l}_j \right) \right) \tag{14}$$

MoreoverFurthermore, we use the Monte-Carlo variance component estimation (MCVCE) to estimate the appropriate variance factors of for different observation groups and the regularization parameter (Koch and Kusche, 2002; Kusche, 2003; Wu et al., 2017c).

3. Numerical results and discussion

The network design of the multilayer model contains several key parameters, like such as the number of layers, the depth of each layer, and the number of Poisson wavelets in each layer. Since the different layers are linked to the anomaly sources located at different depths,s, and the wavelet decomposition is used to separate and extract the contributions from of the different anomaly sources. Moreover, the signal analysis is applied tofor determinening the number of multiply multiple layers based on the background knowledge of local gravity field signals, while, the power spectrum analysis is used to estimate the average depth of each layer. After thatThen, we use a trial and error approach to determine the optimal number of Poisson wavelets in each layer. The wholeA flowchart for designingrepresenting the design of the multilayer model is shown in Figure 1, and the details will be discussed in Sections 3.1 and 3.2.

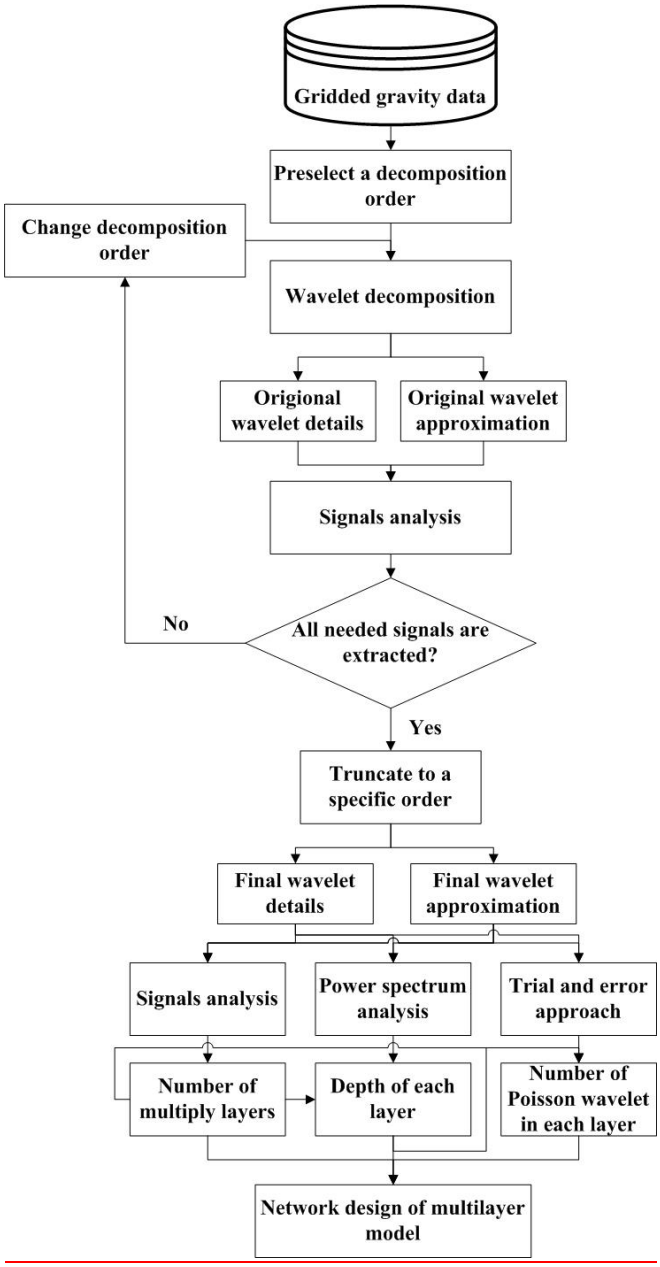

Figure 1 Flowchart ~~for designing~~showing the design of the multilayer model

3.1. Wavelet analysis of local gravity signals

~~In order t~~To determine the depths of the different layers, the residual gravity data are decomposed into ~~the~~ signals at the different scales based on wavelet analysis. ~~The s~~Spline interpolation is used to compute the gridded data, and Coif3 basis functions are chosen for wavelet decomposition (Xu et al., 2017). The preliminary maximum order for wavelet

decomposition is arbitrarily chosen to some extent. However, since ~~the~~ low-order wavelet details are ~~invariant with the~~constant despite ~~increase~~ change ~~of~~ in the decomposition order, we can preliminarily choose a predefined order and implement ~~the~~ wavelet decomposition~~;~~, ~~and~~ we then analyze the derived details in order to choose the optimal order. ~~If~~ For ~~there are still details~~signals ~~that are~~ useful for constructing the multilayer model that ~~haven't been~~ remain~~ed~~ unseparated, we ~~need to increase~~ change the decomposition order until all the useful ~~details~~ signals have been extracted.~~,~~ ~~;~~ ~~o~~Oo~~therwise~~, we truncate to a specific order~~,~~ and compute the wavelet details and approximation to ~~construct~~ conduct the multiple~~y~~ layers~~'s~~ ~~parameterization~~network design. By trial and error~~s~~, the preliminary order for decomposition is chosen as nine~~.~~, ~~and~~ Figure 2 shows the derived wavelet details (the corresponding statistics are provided in Table 1). With the increase ~~of~~ in the decomposition order, more long-wavelength features occur. ~~More~~ S~~s~~pecifically, the low-order wavelet details ~~demonstrate the~~indicate high-frequency signals stemming~~ed~~ from ~~the~~ shallow and small-scale substances~~,~~~~;~~ while~~,~~ ~~the~~ high-order ~~ones~~ wavelet details with long-wavelength patterns reflect ~~the~~ anomalies caused by deep and large-scale geological bodies. ~~It is noticeable that t~~The 1st- and 2nd-order details (~~i.e.,~~i.e. D_1 and D_2) ~~are~~ seem~~s~~ to be dominated by ~~the~~ high-frequency signals that correlate strongly with the local topography (the local digital terrain model (DTM) can be seen in Figure 1 in Wu et al. (2017c)). We ~~mainly~~ attribute this to the uncorrected topographical signals in the RTM corrections~~;~~, ~~which~~ these ~~is~~ remain ~~mainly~~ due to the inaccuracy of the density parameters in RTM and the limitations of DTM ~~both~~ in terms of spatial resolution and precision. As a result, ~~the~~ high-frequency signals originating~~d~~ from local ~~topography~~ topographical variations cannot be thoroughly recovered from RTM reduction, and consequently, the uncorrected signals leak into the 1st- and 2nd-order details. To avoid these high-frequency errors propagating into the final solution, we neglect these two wavelet details in designing the network of multilayer model~~pley layers' networks~~. ~~Moreover, with the order increasing to nine~~With nine layers, we ~~notice~~observed D_9 ~~obviously~~ reveal ~~the~~ large-scale signals with ~~the~~ wavelengths~~hs~~ of hundreds of kilometers. Given that the mean distance between ~~the each pair of~~measured gravity data in this target area is approximately ~~several~~ 6~7 km ~~–~~and the spatial resolution of the applied GGM (~~i.e.,~~i.e. GOCO05S) is roughly 72 km, the spectral contents of the residual signals ~~need~~ to be recovered is roughly between several kilometers and tens of kilometers within the RCR framework~~,~~ ~~– This is, i.e.,~~i.e. approximately between degree 250 to 3000 in terms of spherical harmonic~~s's~~ representation. T~~While, t~~he spectral contents of the 9th-order wavelet details exceed the frequency bands of the signals ~~need~~ to be modeled, ~~and the~~thus, the maximum order for wavelet decomposition is

truncated to eight. In this manner, the third- to eighth-order (D_3 - D_8) wavelet details and the final approximation (A_8) (see the information in Figure 3 and Table 2) are applied for constructing the multilayer model; the model then, consists of seven layers at various depths.

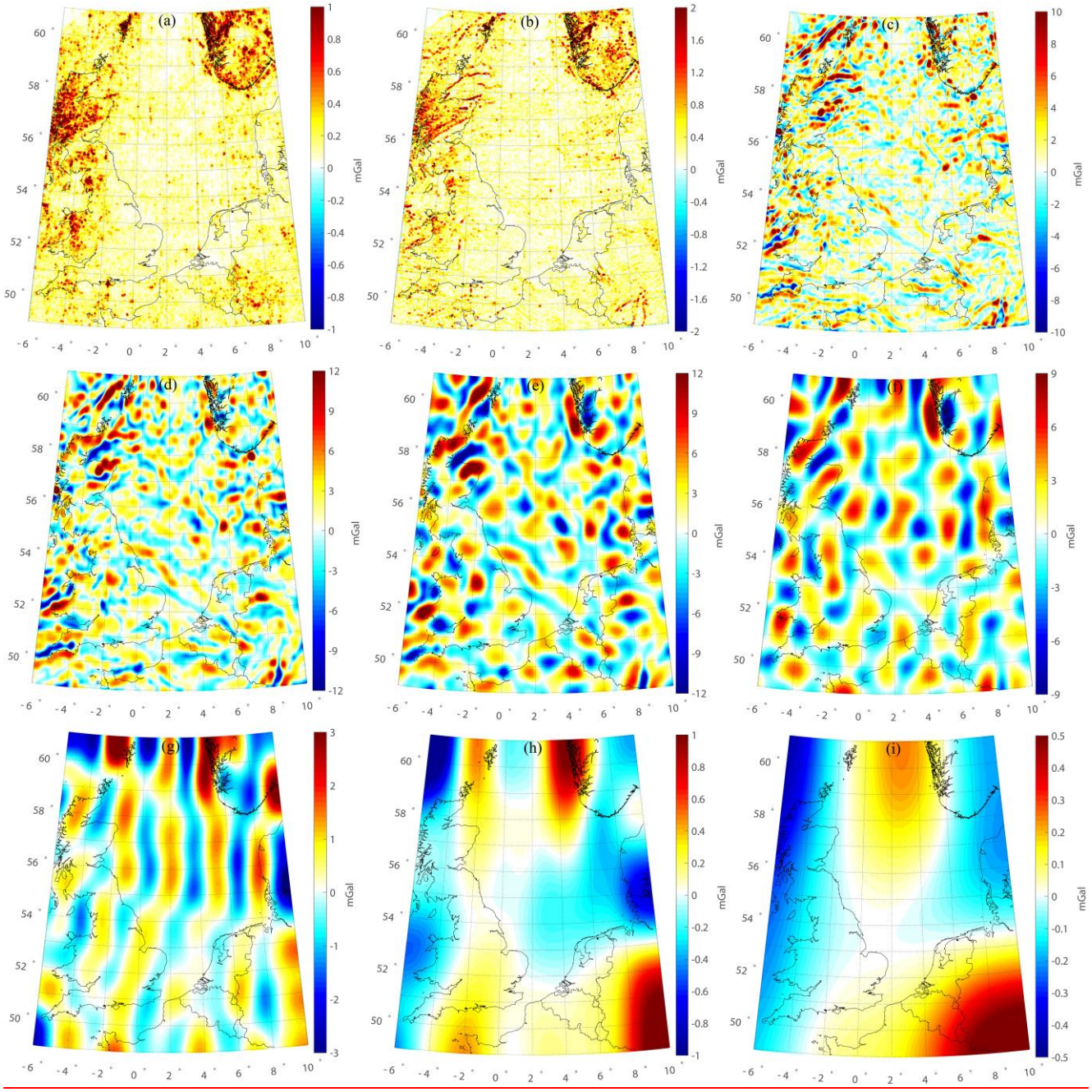

Figure 2. Wavelet details at various scales. (a) D_1, (b) D_2, (c) D_3, (d) D_4, (e) D_5, (f) D_6, (g) D_7, (h) D_8, and (i) D_9.

Table 1. Statistics of different wavelet details (units: mGal)

	Mmax	Mmin	Mmean	Sd
D_1	2.23	-2.78	0.00	0.20
D_2	4.52	-5.57	0.00	0.32
D_3	19.27	-16.26	0.00	2.30
D_4	21.71	-17.46	0.00	3.18
D_5	15.38	-16.47	0.00	3.80
D_6	10.60	-9.72	0.00	2.75
D_7	4.43	-3.33	0.00	0.95
D_8	1.23	-1.52	0.00	0.34
D_9	0.66	-0.45	0.00	0.18

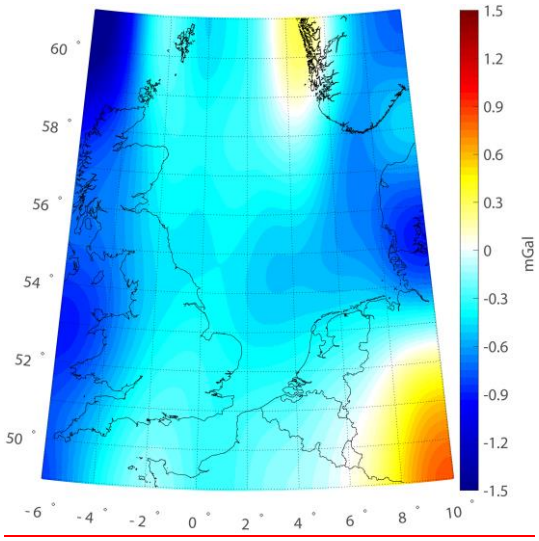

Figure 3. Wavelet approximation A_8 .

Table 2. Statistics of wavelet approximation (units: mGal).

Mmax	Mmin	Mmean	SDsd
0.83	-1.70	-0.41	0.32

3.2. Key parameters of Poisson wavelets

The order of Poisson wavelets is fixed at 3 to achieve a good compromise between the localization in the space and frequency domains (Panet et al., 2011). In addition, the depth and number of Poisson wavelets are the crucial points factors affecting the solution quality of the solutionregional solution (Klees et al., 2008). Poisson wavelets belonging to different layers are placed on the Fibonacci grids at various depths beneath the topographyEarth's surface, and the power spectrum analysis is applied to estimate the depths. As shown iIn Figure 4, the green curves show the radially averaged logarithm power spectrums of signals at different scales, and the red straight lines represent the slopes of the spectrums, indicate indicating the depths of the corresponding layers. The red lines represent the rates of change for logarithmic power relative to the wave number, estimated by an autoregressive method.; and theThe starting pointinitial and terminal points of the red lines are the inflection points of the curves, recognized according to the trend of the curves (Xu et al., 2018). The layers go deeper as the scales increase, and the shallow layers reflect the small-scale signals, while the deep ones recover the long-wavelength information. Table 3 provides the estimated depths of the different layers, limited between 4 and 60 km. The shallowest layer wasis locates located 4.5 km

underneath the ~~topography~~Earth's surface, while the ~~depth of the~~ deepest ~~one~~ layer is ~~approximately~~ estimated ~~as~~ to be approximately 59.2 km below the Earth's surface. ~~It is noticeable that t~~The thickness of the sediments in ~~this~~ the study area is approximately 2~4 km, and the thickness of the upper-middle crust is roughly 15~20 km (Artemieva and Thybo, 2013). Thus, the first four layers (layer_1, layer_2, layer_3, and layer_4) are located between the sediments and upper-middle crust~~, and~~ T~~t~~he corresponding wavelet details (D_3 , D_4 , D_5 , and D_6) ~~display as the~~comprised~~d~~ small-scale patterns due to the highly heterogeneous structure of the crust. D_3 and D_4 correspond~~ed~~ to the tectonic structure in the upper crust. The distributions of D_3 and D_4 (~~with~~ at the average depths of 4.5 km and 9.2 km, respectively) on land are more dispersed than that in the ocean, and ~~demonstrate that~~ the tectonic structure underneath the land is found to be more complex than that beneath the ocean in the upper crust. Moreover, the gravity anomalies in the northern part of North Sea are more dispersed than those in the central and southern parts of North Sea, which is consistent with the fact that the Viking Graben and two basins (i.e. Forth Approaches Basin and Norwegian-Danish Basin) are located in the northern and southern parts of North Sea, respectively~~,~~ (~~e.g.,~~e.g. see Fichler and Hospers (1990), and Blundell et al. (1991)). The mean source depths of D_5 and D_6 are 13.7 km and 19.6 km, respectively; they~~,~~ correspond to the depth~~s~~ of the middle crust. The gravity anomalies ~~during~~ in these two layers present apparent positive-negative alternating patterns, which may be interpreted as the crustal shearing and extrusion (Blundell et al., 1991; Ziegler and Dèzes, 2006). ~~While, t~~The last three layers (layer_5, layer_6, and layer_7) ~~are supposed to be~~were~~are~~ assumed to be located between the Moho surface and upper mantle, considering that the Moho depth in ~~this~~ the region is approximately 25~30 km (Grad and Tiira, 2009), and the corresponding details (D_7 , D_8 , and A_8) become smoother and more long-wavelength signals occur. D_7 , with ~~the~~ a mean source depth of 27.0 km primarily reflects the Moho undulation. The distribution of positive-negative alternating gravity anomalies in D_7 is nearly south-north oriented, which is in agreement with the features of the Moho relief in ~~this~~ the area (Fichler and Hospers, 1990; Ziegler and Dèzes, 2006). The average source depths of D_8 and A_8 are 32.3 km and 59.0 km, respectively, corresponding ~~with~~ to the depth of the upper mantle;~~,~~ this indicates that the density distribution of the upper mantle is relatively smooth. Overall, these decomposed gravity anomalies can reveal the tectonic structure of the study area at different depths.

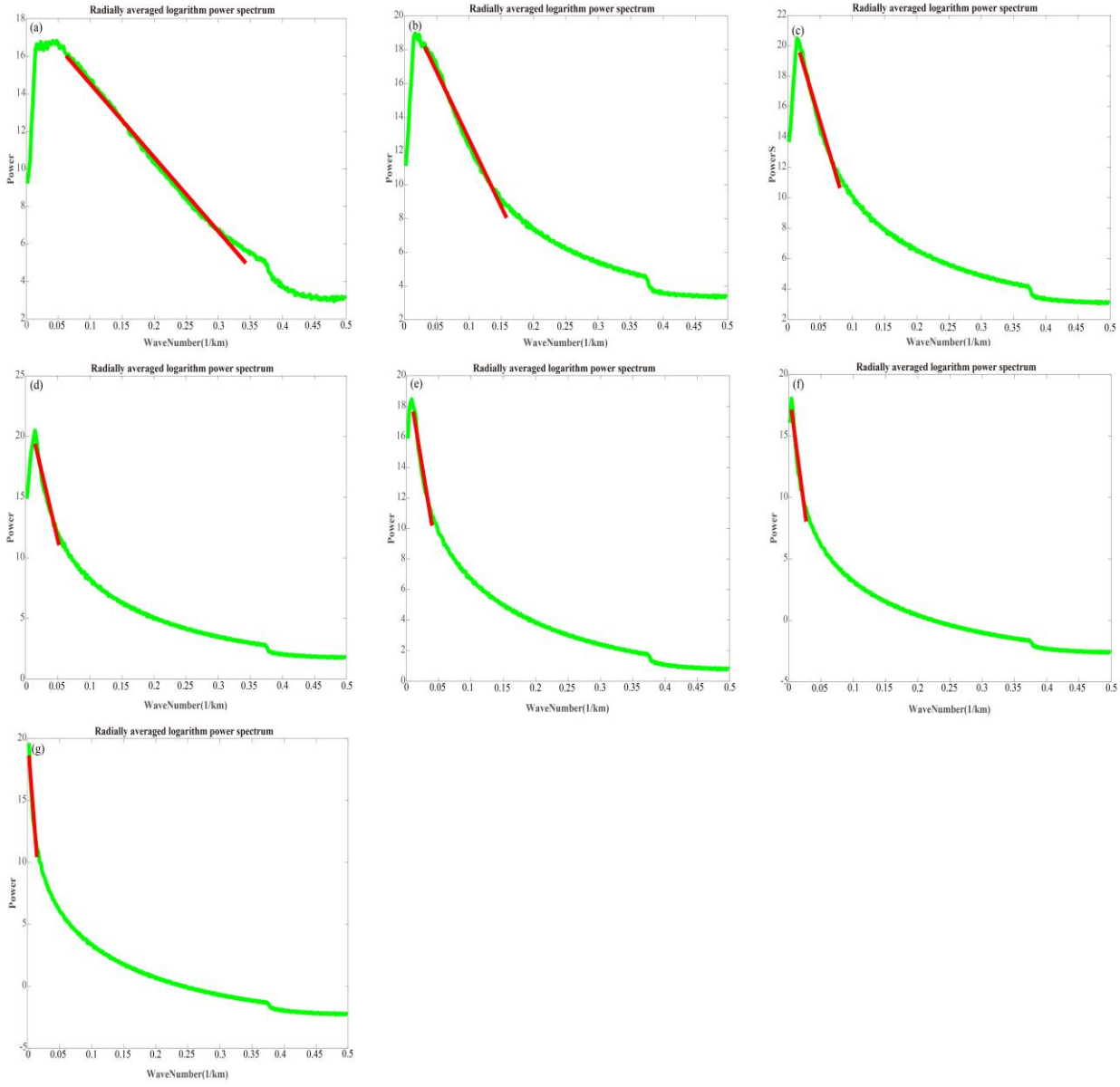

Figure 4. Power spectrum analysis of various wavelet signals. (a) D_3, (b) D_4, (c) D_5, (d) D_6, (e) D_7, (f) D_8, and (g) A_8.

The green curves are the radially averaged logarithm power spectrums, and the red straight lines represent the rates of change for logarithmic power relative to wave number.

Table 3 Depths of the ~~multiply~~ multiple layers beneath the ~~topography~~ Earth's surface (Units: km).

layer 1	4.5
layer 2	9.2
layer 3	13.7
layer 4	19.6
layer 5	27.0
layer 6	32.3
layer 7	59.2

~~As mentioned above, different layers are designed to recover the wavelet details and approximation at different scales, and A~~a trial-and-error approach is used to estimate the number of Poisson wavelets ~~of~~ at each layer (Wittwer, 2009). For a specific layer with ~~the~~ a fixed depth, we predefine~~d~~ different numbers of Poisson wavelets to form a certain number of Fibonacci grids. Then, the signals reconstructed from these grids are compared with the true values, ~~i.e.,~~i.e. ~~ones~~ those derived from wavelet decomposition~~.~~, ~~and t~~The parameter that ~~derives~~ obtains the smallest difference~~s~~ between the modeled and true signals is consider~~ed~~ as the optimal ~~one~~parameter. By tr~~a~~ial and error~~s~~, the spatial resolutions of the Fibonacci grids (mean distance between Poisson wavelets) are changed from 20 to 14 km with a step of 1 km. Table 4 shows the accuracies of the solutions derived from the different Fibonacci grids of the ~~multiply~~ multiple layers, and we take the situation of the first layer for instance. With ~~the~~ increase ~~of~~ in the number of Poisson wavelets, the ~~SD value~~standard deviation of the differences between the reconstructed and true signals decreases gradually to 0.12 mGal when the spatial resolution of the grid increase~~s~~ to 16 km. ~~Since then~~Beyond this point, no significant ~~improvements~~ changes occur ~~with~~ on incorporating more Poisson wavelets. Moreover, introducing more Poisson wavelets increases the overlapping between them, which may lead to ~~the~~ highly-conditioned normal matrices, and the associated heavy regularization may decrease the solution quality (Wu et al., 2017b). The optimal mean distance between Poisson wavelets of the first layer is estimated as 16 km. Similarly, the spatial resolutions for the ~~rest~~ remaining layers can be determined in this way~~,~~ (see Table 4).

Table 4 Accuracies of solutions derived from the various Fibonacci grids ~~of~~ for different layers (Units: mGal).

	20 km	19 km	18 km	17 km	16 km	15 km	14 km
l~~L~~ayer 1	0.43	0.34	0.21	0.16	0.12	0.12	0.12
l~~L~~ayer 2	0.52	0.43	0.33	0.25	0.19	0.16	0.16
l~~L~~ayer 3	0.58	0.40	0.28	0.19	0.16	0.14	0.14
l~~L~~ayer 4	0.55	0.39	0.29	0.26	0.15	0.13	0.13
l~~L~~ayer 5	0.38	0.26	0.17	0.14	0.10	0.10	0.10
l~~L~~ayer 6	0.22	0.16	0.12	0.10	0.08	0.08	0.08
l~~L~~ayer 7	0.11	0.09	0.08	0.06	0.06	0.06	0.06

3.3. Regional solution and its validation

For regional gravity field recovery, point-wise terrestrial and ~~shipboard~~shipborne gravity anomalies ~~are~~ are~~were~~ combined. Since there is~~was~~ ~~are~~ no accurate information on the ~~accurate~~ accuracies~~y~~ ~~information for~~ of terrestrial and ~~shipboard~~shipborne data, we assume~~d~~ ~~the~~ an ~~accuracies~~ accuracy of 2 mGal for both of these ~~two~~ types of data, and the posterior variance factors of different ~~observation groups~~data ~~are were~~are estimated from MCVCE ~~method~~. The weights of different ~~observation groups~~data~~,~~ indicate their relative contributions, and play a key role in data combination. The estimated variance factors for terrestrial and ~~shipboard~~shipborne gravity data ~~are were~~are approximately 1.45 mGal and 1.30 mGal, ~~through the MCVCE method,~~ respectively, when we model~~led~~ the local gravity field based on the multilayer approach. For terrestrial data, the estimated accuracy ~~is in good agreement~~agree~~s~~d with that derived by Klees et al. (2008), ~~i.e.,~~i.e. 1.48 mGal for parts of the Netherlands. However, it is difficult to judge whether this estimate ~~is was~~is realistic in other regions, because of a lack of accuracy information. ~~While, f~~For ~~shipboard~~shipborne data, the computed value of 1.30 mGal is smaller than the results of crossover adjustments, where the standard deviation for the residuals at the crossovers was ~~approximately~~ estimated ~~as~~ to be approximately 2.0 mGal (Slobbe, 2013). However, this value may be too optimistic, considering that much of the shipborne data were collected decades ago without GPS navigation. The first-order Tikhonov regularization is used to tackle the ill-conditioned problem (Kusche and Klees, 2002; Wu et al., 2017b), and the convergent regularization parameter is ~~was~~ estimated to be approximately 0.5×10^{-5} ~~estimated from~~using the MCVCE method~~; ~~. For the d~~~~D~~etails ~~for~~ on regularization parameter estimation and comparisons with different methods can be referred to Wu et al. (2017b).

The performance of the ~~traditionally used~~ single-layer approach is also investigated for comparison~~, –. and t~~The parameterization of the local gravity field based on the single-layer approach ~~can be seen in~~has been described in detail by ~~, e.g.,~~e.g. Klees et al. (2008) and Slobbe (2013). By trial and error~~s~~, the single layer of the Poisson wavelets' grid ~~is~~ ~~was~~is found to be located 40 km beneath the Earth's surface~~topography~~, and the mean distance between the Poisson wavelets ~~is was~~is defined as 8.7 km (Wu et al., 2016b). Figure 5 shows the normalized ~~spectrums~~ spectrums~~a~~ for different approaches. Considering the frequency range of the signals to be recovered in the target area is approximately between degree 250 to 3000 in spherical harmonics~~s'~~ representation, we note the single-layer approach is only sensitive to a part~~s~~ of the signal~~s'~~ spectrum. It ~~was~~is sensitive~~, i.e.,~~ approximately between degree 300 to 1200 if we ~~suppose~~ assume the criterion for determining whether it is sensitive or not within a specific frequency band to be half of the maximum value of the normalized spectrum ~~is the criterion for determining whether it is sensitive or not within a specific frequency band~~. However, for the high-frequency band between degree 1200 to 3000, this approach is less sensitive. On the contrary, the multilayer approach effectively covers the spectrum of the local gravity signals, ~~which is~~and ~~was~~is ~~both~~ sensitive to both the low- and high-frequency bands. The residuals of data after least squares adjustment using different methods are displayed in Figure 6~~.~~ (the boundary limits for this area are contracted by 0.5 ° in all the directions to reduce edge effects)~~, shows the~~The residuals derived from the multilayer approach ~~were~~are ~~reduce~~ significantly lower ~~in the whole~~throughout the region compared with ~~ones~~ those obtained from the single-layer approach, especially in the western parts of UK, south of Norway, and southwest parts of Germany. In these regions~~, where the~~ high-frequency signals that are correlated with local topography dominate the ~~features of~~ regional gravity field. We also ~~find the~~noted improvements ~~occurring~~ in the oceanic parts, especially in the waters around the English Channel, Irish Sea, northwest of the North Sea, and the Atlantic Ocean close to northwest UK. ~~The statistics in~~ Table 5 displays the standard deviation (SD) value for the residuals of terrestrial (shipborne) gravity anomalies, which decreases by 0.37 mGal (0.34 mGal) when the multilayer approach is used. These results are reasonable, since the multilayer ~~approach~~ model contains several layers shallower than 40 km, and the spectrums of these layers shift to the high-frequency bands. ~~As a result~~Thus, the spectrum of the multilayer approach ~~is was~~is more sensitive to ~~signals with~~ high-frequency ~~properties~~signals, and consequently, the local high-frequency signals ~~can could~~can be better fitted by the multilayer approach. It is also worth ~~to~~ mentioning that the analysis of data residuals ~~can't~~ cannot be treated as the only ~~criteria~~ criterion ~~for~~ to justify~~ing~~ the performances of different approaches. There are two major reasons for this~~,~~ First, ~~since~~ these gravity data have been used for modeling purposes, and the SD values of data residuals should be

regarded as the internal agreement. Additionally, ~~Besides,~~ due to the limitation of the accuracies of gravity data, we ~~can't~~ cannot ~~make~~ arrive at firm conclusions ~~too firmly~~ based only ~~depends~~ on the analysis of data residuals. ~~One may also argue that it may be possible to derive~~ It is also possible that lower data residuals ~~could~~can be derived if we ~~put~~ place the Poisson wavelets' grid at a shallower depth when the single-layer approach is used. However, we think~~believe~~ a shallower single grid may reduce the data residuals, but may not derive a better solution when validated against the independent control data, ~~see the~~as described in detail by ~~detailed discussions in~~ Wu et al. (2016b). In the following part, we introduce another high-quality independent data set for external validation, ~~i.e.,~~i.e. GPS/leveling data, ~~for external validation,~~ which gives us more confidences with respect to the performances of different methods.

It is also of interest to implement an Akaike information criterion (AIC) test for different models. Although, the multilayer model fits the gravity observations better, ~~but~~ it also increases the level of estimated parameters. AIC rewards the goodness of fit of data, but also includes a penalty ~~with~~ as ~~the increasing of~~ the number of estimated parameters increases. In other words, it deals with the trade-off between the goodness of fit of the ~~model~~ data and the simplicity of the model. The AIC value is an estimator of the relative quality of statistical models for a given set of data, providing a means for model selection~~,~~. ~~and t~~The model that ~~gives~~ yields the minimum AIC value may be more preferable (Akaike, 1974; Burnham and Anderson, 2002). The definition for the AIC value can be seen in e~~E~~q. (A1) in the Appendix. Since we model the gravity field in the framework of least squares system, we can simply take $AIC = 2k + m\ln(RSS/m)$ for model ~~comparision~~comparison, where k is the number of estimated parameters in the model, m is the number of observations, and RSS is the residual sum of squares (RSS~~),~~). For details, see ~~the details in~~ the Appendix. In this study, 894649 ~~the number of~~ point-wise gravity observations ~~were~~are used for ~~modeling~~modeling ~~is 894649~~, and 47504 and 19477~~the numbers of estimated~~ parameters ~~were~~are estimated in the multilayer and single-layer model~~s, are 47504 and 19477,~~ respectively. The RSS values for the multilayer and single-layer model ~~wa~~~~e~~~~re~~are computed as $8.8527\times10^{5}\ mGal^{2}$ and $1.3296\times10^{6}\ mGal^{2}$, respectively, based on the data residuals after the least squares adjustment. Then~~,~~, the AIC values for the multilayer and single-layer model ~~are~~ ~~were~~are estimated as 85581 and 393400, respectively. Based on these statistics, we not~~ice~~e that the multilayer model ~~gives~~ yields a smaller AIC value, which may be more preferable ~~since~~ because it ~~reaches~~ achieves a better balance between the goodness of fit of the data and the simplicity of the model.

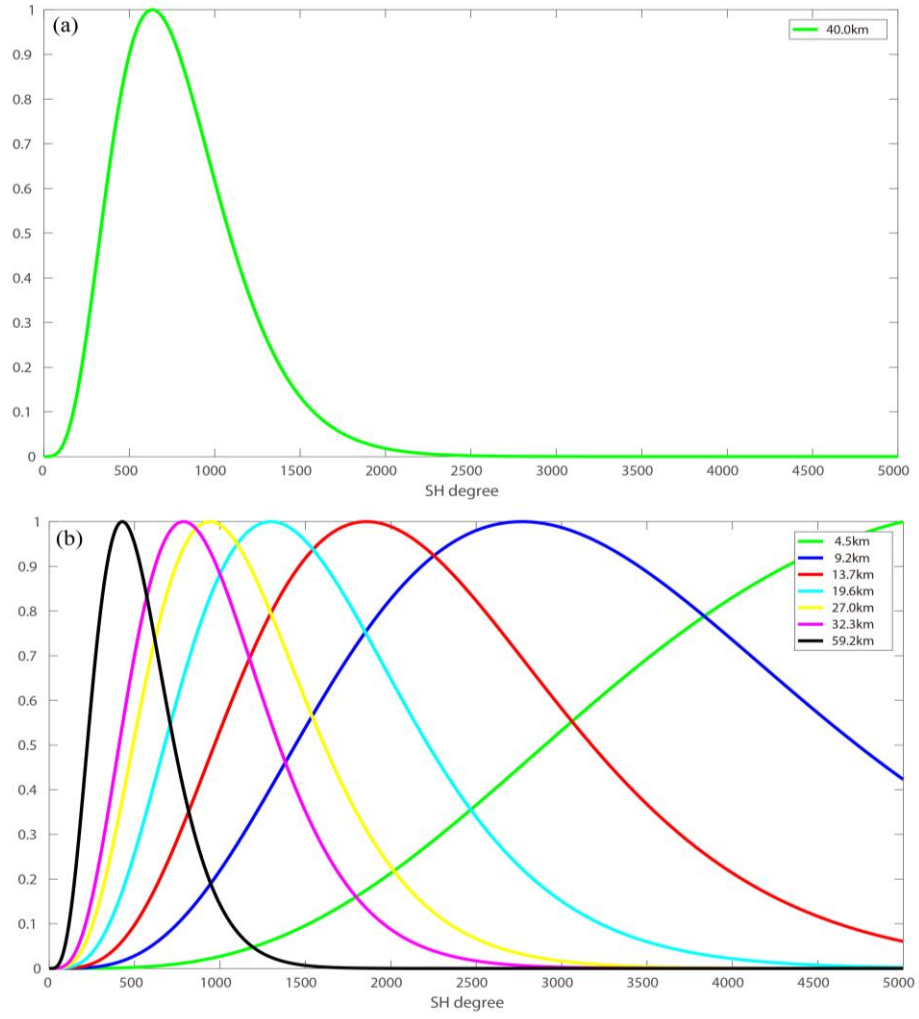

Figure 5. Normalized ~~spectrums~~ spectrum for (a) single-layer and (b) multilayer approach.

To test the ability of realistic extrapolation of different regional models recovered from various methods, we introduce GPS/leveling data in the Netherlands (534 points), Belgium (2707 points), and parts of Germany (213 points) as the independent validation data. This is a comparison of~~which is actually comparing~~ the predicted values derived from the regional model (~~e.g.,~~e.g. model computed from the multilayer or single-layer approach) and ~~ones~~ those derived from independent survey/measurements.~~,~~ ~~we introduce GPS/leveling data in the Netherlands (534 points), Belgium (2707 points), and parts of Germany (213 points) as the independent validation data.~~ These data ~~are~~ were provided in terms of geometric quasi-geoid heights derived from the high-quality GPS measurements and leveling surveys.~~, and~~

Tthe overall estimated accuracy of these observed quasi-geoid heights is was approximately at the 1 cm level. It is worth to mentioning that these GPS/leveling data are werehave not been combined for modeling, and their three dimensionalthree-dimensional coordinates don'tdiddo not coincide with the positions of gravity data. For validating different models with GPS/leveling datapurposes, we needit is necessary to reconstruct the regional model based on the computed estimated Poisson wavelets' coefficients and coordinates of GPS/leveling points (see Eq.(12)), and compute the gravimetric quasi-geoid heights at these predicted points., which are ones predicted from the regional model. Then, Wwe then compute the standard deviation (SD) of the point-wise difference between GPS/leveling data and the gravimetric quasi-geoid height derived from the regional approach. This, which servesd as an is actually external validation.

The validation results demonstrate that the discrepenciesdiscrepancies between the GPS/leveling points and quasi-geoid heights derived from the multilayer approach decrease substantially compared with ones those computed from the single-layer approach , see (Figure 7). The most prominent improvements occur in the northwest of Belgium, west of Germany, and eastern parts of Netherlands, which are in good agreement with the results for data residuals analysis demonstrated in Figure 6. As shown in Table 6, the accuracies of gravimetric quasi-geoid derived from the multilayer approach are improved by 0.4 cm, 0.9 cm, and 1.1 cm in the Netherlands, Belgium, and parts of Germany, respectively. Moreover, the mean values indicate that the solution computed from the multilayer approach further reduces the biases between the gravimetric solution and local GPS/leveling data, with the magnitudes of 0.8 cm, 0.7 cm, and 1.1 cm in these three regions, respectively, compared to the one those modeled from the single-layer approach. From these results, we can see that the multilayer approach not only leads to a reduction for the data residuals, but also generatesderives a better solution assessed by the independent control data, compared to the single-layer approach. For To constructing the multilayer model, we considered that the gravity signals are the sum of the contributions generated from the anomaly sources, and different layers are designed for recovering these contributions with heterogeneous spectral contents. As a result, the spectrum of the multilayer approach is sensitive to the frequency bands of local gravity signals, both in the low- and high-frequency bands, and the local signals may have beenbe better recovered. We also notice that there are still biases between the regional gravimetric solutions and local GPS/leveling data, (see the mean values in Table 6), which are mainly due to the commission errors in the GGM and uncorrected systematic errors in the local gravity data and leveling systems (Fotopoulos, 2005). Generally, corrector-surface (Fotopoulos, 2005; Nahavandchi and Soltanpour, 2006) or more complicated algorithms, like least squares collocation (Tscherning, 1978),

boundary-value methodology (Klees and Prutkin, 2008; Prutkin and Klees, 2008), and a direct approach (Wu et al., 2017a), can be applied to reduce the systematic errors and properly combine GPS/leveling data and gravimetric solutions. However, since the objective~~target~~ of~~for~~ this study is to develop a multilayer approach for gravimetric quasi-geoid modeling~~,~~ that ~~would~~may be served ~~which is served~~ as a ~~basic~~ basis ~~surface~~ for further geophysical applications, the derived quasi-geoid ~~was~~is not purely gravimetric with implementing the data merging approach~~.e.g., study the ocean circulation and structure of lithosphere; while, after implementing these methods for combining local GPS/leveling and gravimetric model, the derived quasi-geoid is not purely gravimetric~~. Furthermore ~~Besides~~, we only have ~~the~~ well distributed GPS/leveling data in ~~the~~ a limited region, ~~i.e.,~~i.e. in the Netherlands, Belgium, and parts of Germany, while in other regions, no high-quality control data are available. If we use the locally distributed GPS/leveling data ~~for~~ to ~~removing~~ remove these systematic errors and computing the combined quasi-geoid, the final solution may ~~have been~~be distorted in other regions, especially around~~in~~ the ocean ~~parts~~, ~~since~~ because no control data ~~was used~~exist in the~~se~~ese regions ~~have been combined~~. Thus, we ~~don't did~~o not implement the~~se~~ methods mentioned above for computing the combined quasi-geoid. ~~In following study, w~~We use the gravimetric model derived from the multilayer approach for the following study, which is hereafter denoted as QGNSea V1.0 (quasi-geoid over the North Sea version 1.0).

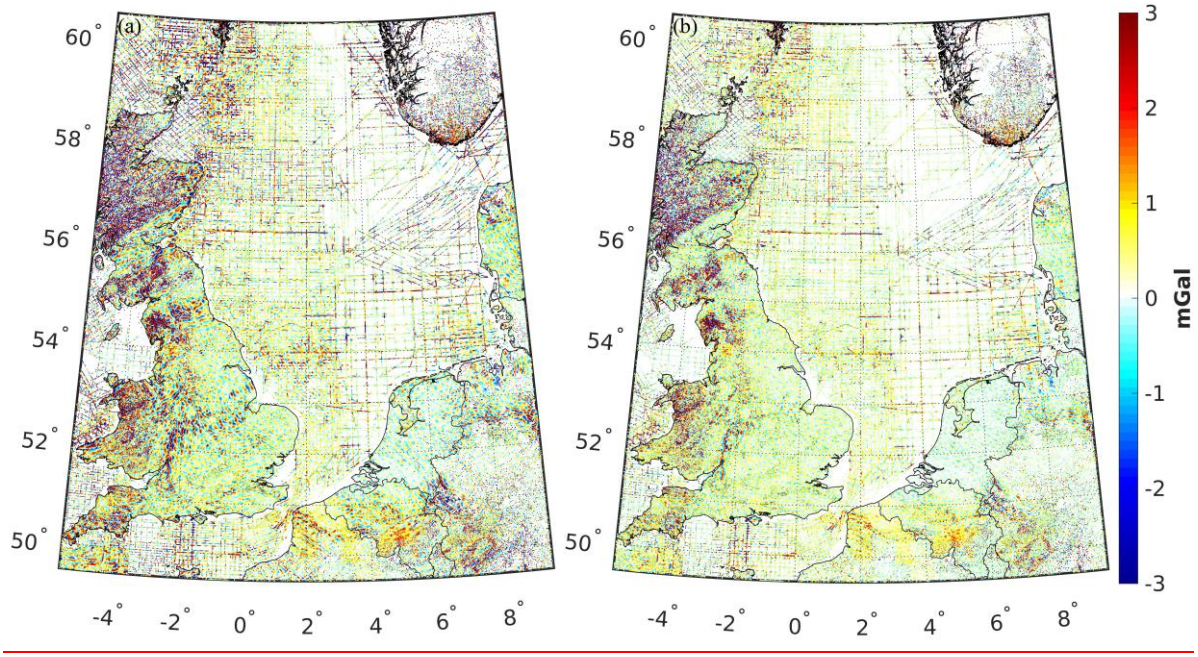

Figure 6. Residuals of gravity data derived ~~from~~ using the (a) single-layer and (b) multilayer approach.

Table 5 Statistics of residuals of gravity data computed ~~from~~ using different approaches (units: mGal).

		M~~m~~ax	M~~m~~in	M~~m~~ean	SD~~sd~~
Single-layer approach	Terrestrial	19.58	-16.91	0.00	1.37
	Shipborne	11.91	-17.38	0.00	1.02
Multilayer approach	Terrestrial	16.96	-14.90	0.00	1.00
	Shipborne	9.25	-15.96	0.00	0.68

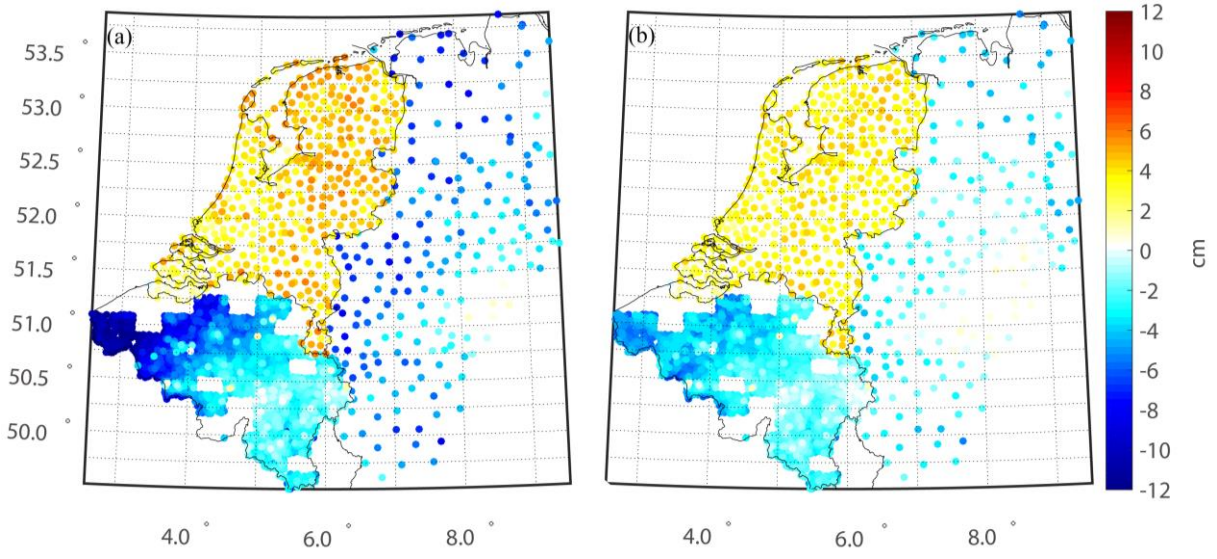

Figure 7. Differences between GPS/leveling data and gravimetric quasi-geoids computed using ~~from~~ the (a) single-layer and (b) multilayer approach.

Table 6 Evaluation of gravimetric quasi-geoids modeled ~~from~~ using different approaches (Units: cm).

		Max	M~~m~~in	M~~m~~ean	SD~~sd~~
Single-layer approach	Netherlands	5.9	0.1	3.8	1.2
	Belgium	1.2	-13.1	-3.5	2.8
	Germany	1.2	-11.2	-3.6	2.9
Multilayer approach	Netherlands	4.8	0.0	3.0	0.8
	Belgium	1.2	-6.8	-2.8	1.9

Germany	1.0	-6.7	-2.5	1.8

QGNSea V1.0 is compared with a regional model called EGG08 (Denker, 2013), and ~~other~~ four other recently published high-order GGMs, ~~i.e.,~~i.e. EGM2008 with ~~the~~ a full degree and order (d/o) of 2190 and 2159 (Pavlis et al., 2012), EIGEN-6C4 (d/o 2190) (Förste et al., 2014), GECO (d/o 2190) (Gilardoni et al., 2015), and SGG-UGM-1 (d/o 2159) (Liang et al., 2018)~~, for further comparisons~~. The reason for choosing these four GGMs for comparisons is that these models have relatively higher spatial resolutions and better accuracies compared to most ~~of~~ other available GGMs~~,~~ (see the information in http://icgem.gfz-potsdam.de/home). EGG08 is a regional gravimetric quasi-geoid model in Europe, which was recovered by ~~stokes~~ Stokes' integral based on locally distributed gravity data. This model is provided in terms of gridded data instead of spherical harmonics, and its ~~the space~~ spatial resolution ~~of which~~ is 1′ in latitude and 1.5′ in longitude, respectively (Denker, 2013). ~~While, t~~The other~~rest~~ four models are global geopotential models provided in terms of spherical harmonics, and EGM2008 was computed by merging GRACE measurements, terrestrial, altimetry-derived, and airborne gravity data. Since no GOCE data have been incorporated for developing EGM2008, and the recently published GGMs have been developed by combining GOCE data, which is supposed to improve the gravity field in the frequency bands approximately from degree 30 to 220 in spherical harmonics representation (Gruber et al., 2010). EIGEN-6C4 was computed by combining GRACE, GOCE, and terrestrial gravity data and other data sets; GECO was computed by incorporating the GOCE-only TIM R5 (d/o 250) solution into EGM2008, and SGG-UGM-1 was computed by the combination of EGM2008 gravity anomalies and GOCE gravity gradients and satellite-to-satellite tracking data. The ~~Differences~~ differences between QGNSea V1.0 and other models are shown in Figure 8 (the boundary limits for the area are ~~contracted~~ reduced by 0.5 ° in all ~~the~~ directions to reduce edge effects), the magnitude of which reaches the decimeter level. For EGG08, we note the most prominent differences appear in the eastern parts of the Irish Sea and center of Germany. Different data pre-processing procedures and methods for parameterization partly account for these differences. For example~~,~~ ~~e.g.,~~ QGNSea V1.0 is recovered from the multilayer approach using Poisson wavelets, and proper weights for different observation groups are estimated through MCVCE~~,~~ while the spectral combination technique and spectral weights were implemented in EGG08 for merging heterogeneous data (Denker, 2013). Larger differences are observed between QGNSea V1.0 and these four GGMs, and remarkable differences are seen~~show~~ in southern ~~of~~ Norway, northern parts of the North Sea, eastern parts of the Irish Sea, and northwest parts of Germany~~.~~ ~~besides from the applications of different techniques for modeling,~~

Tthese differences are partly interpreted as resulting from the different modeling techniques, and the additional signals introduced by QGNSea V1.0, stemming from the incorporation of more high-quality gravity data. The evaluation results with GPS/leveling data displayed in Figure 9 and Table 7 show that the gravimetric quasi-geoid inversed from the multilayer approach has the best quality, especially in the north of the Netherlands and western and eastern parts of Belgium. Note that we removed the mean values between the gravimetric model (both for the regional models and GGMs) and local GPS/leveling data, since these GGMs deviate from the local GPS/leveling data by tens of centimeters or even largermore in this area, due to the commission errors and uncorrected systematic errors in gravity data and inconsistencies among different height datums. Thus, if the mean biases are not removed, these differences are almostcan become dominated by the systematic errors, which is undesirable for model comparisons. The SD value of the misfit between the GPS/leveling data and QGNSea V1.0 is 1.5 cm, while this value increases to 2.2 cm when for EGG08 is validated. In contrast, the accuracies of these four GGMs, approximately at 2.6 cm levels, are slightly worse than that of EGG08, which are approximately at 2.6 cm levels. Compared to these GGMs, the added values introduced by the local high-quality data lead to the primary improvements of in QGNSea V1.0. We find found find that these four GGMs have the comparable accuracies., where tHowever, those he ones developed by combining GOCE data and EGM2008 (i.e.,i.e. GECO and SGG-UGM-1) don't do not have demonstrate better performances than EGM2008 alone, and with SGG-UGM-1 even showinghas the a slightly worse performance than EGM2008., which This is especially particularly prominent in the eastern parts of Belgium., howeverHowever, the possible reasons need require further investigation. We also notice that aA new Europe gravimetric quasi-geoid model, called EGG2015, has beenwasis also observed to have been computed, where the GOCE-derived GGMs were used as the reference models (Denker, 2015). However, this model is not publicly available, and its performance can't cannot be assessed in this local region. It is noticeable that the Ssystematic errors remain in the results shown in can be seen in the results presented in Figure 9. These errors remain because, since these errorsthey cannot be thoroughly removed by simply removing the mean differences. However, as we discuss abovementioned previously, the target for of this study is wasis to develop a multilayer approach for gravimetric quasi-geoid modeling., and iImplementing the data merging approach for combining local GPS/leveling and gravimetric model may derivelead to a distorted solution. Thus, aAnd, the detailed discussion of regarding the removing removal of these systematic errors is out of the scope of this study.

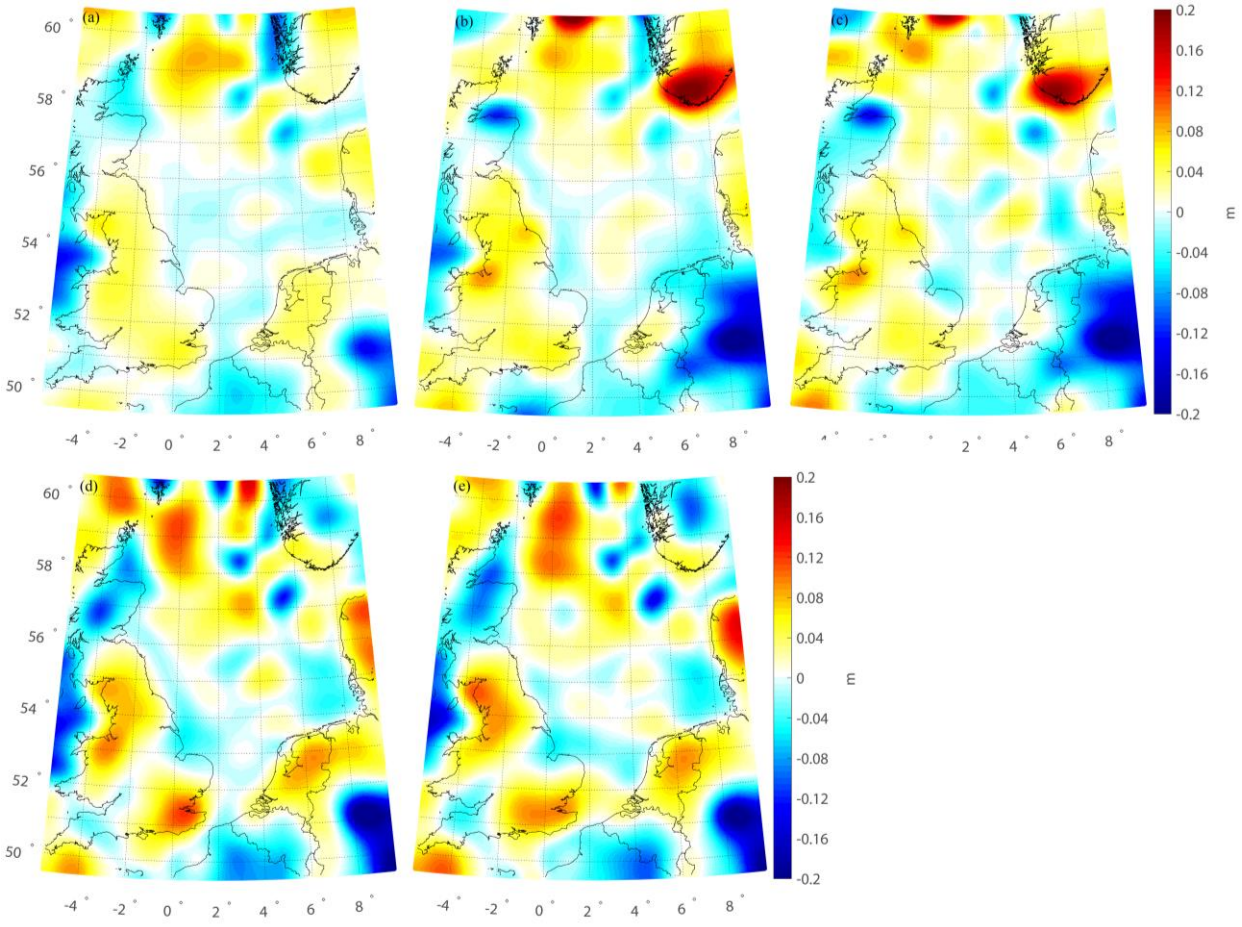

Figure 8. Difference between QGNSea V1.0 and (a) EGG08, (b) EGM2008, (c) EIGEN-6C4, (d) GECO, (e) SGG-UGM-1. Note that the mean differences are removed.

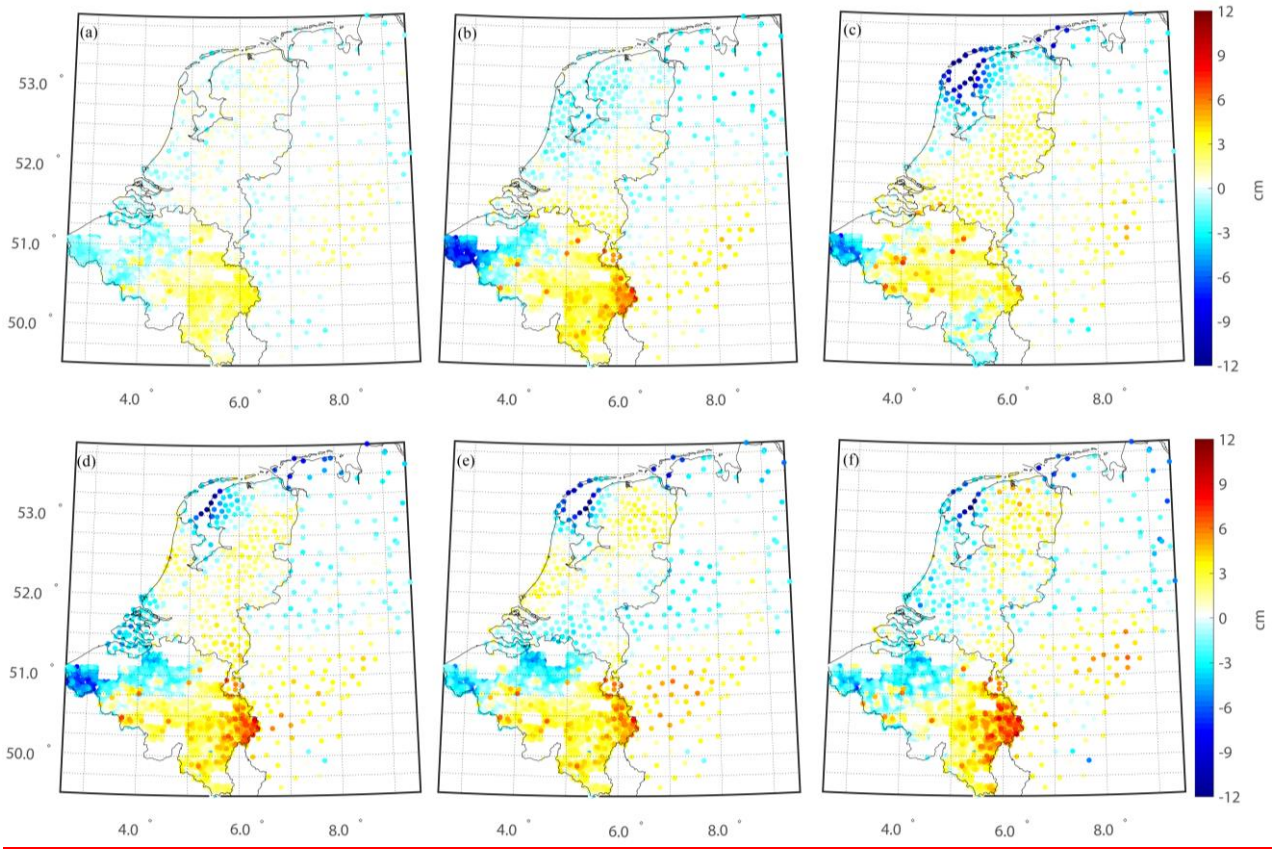

Figure 9. Evaluation of the various gravimetric quasi-geoids. (a) QGNSea V1.0, (b) EGG08, (c) EGM2008, (d) EIGEN-6C4, (e) GECO, and (f) SGG-UGM-1. Note that the mean differences are removed.

Table 7. Statistics of accuracy ~~of~~ for various gravimetric quasi-geoids. (units: cm). Note that the mean differences are removed.

	M~~m~~ax	M~~m~~in	~~sd~~SD
QGNSea V1.0	5.2	-3.9	1.5
EGG08	7.8	-9.4	2.2
EGM2008	8.4	-10.0	2.6
EIGEN-6C4	9.0	-11.9	2.7
GECO	8.3	-12.8	2.6
SGG-UGM-1	8.8	-12.7	2.7

For further comparison~~s~~, we compute the local mean dynamic topography (MDT), which illustrates the departure of the mean sea surface (MSS) from the quasi-geoid/geoid (Becker et al., 2014; Bingham et al., 2014). We compute the MDTs in a geodetic ~~way~~manner, ~~and the~~with raw MDTs ~~are~~ computed as the differences between MSS and local geoid/quasi-geoid models.~~,~~ T~~and t~~he derived MDTs are further smoothed with a Guassian filter to suppress the small-scale signals from the MSS or local geoid/quasi-geoid that ~~can't~~ cannot be resolved ~~from the MSS or local geoid/quasi-geoid~~ (Andersen et al., 2013). The DTU13MSS from 1993-2012 is chosen as the MSS, and this model is provided as the gridded data~~,~~ with ~~the~~ a spatial resolution of 1′×1′ (Andersen et al., 2013). Considering that QGNSea V1.0 and EGG08 have better performances than other models ~~compared with~~when validated against local GPS/leveling data ~~are compared~~, we only compute ~~the~~ local MDTs based on these two gravimetric quasi-geoid models~~s~~. DTU13MSS and QGNSea V1.0/EGG08 are directly combined to obtain the raw MDT. Then, a Gaussian filter with a correlation length of 6 km is further applied to smooth the derived MDT, considering the ~~small scale~~ signals at very short scales ~~that have the wavelengths shorter than several kilometers~~ can~~'t~~ not be recovered from the local gravity data, ~~since the mean distance between gravity data is approximately at 6~7 km level~~due to the limited spatial resolution of the gravimetric measurements.

The ~~modeled~~ MDTs modeled based on QGNSea V1.0 and EGG08 are denoted as MDTNS_QGNSea and MDTNS_EGG08, respectively~~, see~~ (Figure 10). The results of these models agree~~,~~ ~~showing in good agreement~~ with each other in most ~~areas~~ regions over the North Sea. Prominent signals ~~like~~ such as ~~those due to~~ the Norwegian coastal currents can be seen in the~~se two~~ MDTs, ~~obtained from these two models (, also see e.g.,~~e.g. see ~~(~~Idžanović et al.~~, (~~(2017).~~, although~~ T~~t~~he signals observed in MDTNS_QGNSea ~~don't~~ do not provide a full picture of Norwegian coastal currents due to the limited data coverage in Norway and its neighbo~~u~~ring ocean areas. ~~While, i~~In ~~other~~ most areas of the North Sea, the MDTs show ~~quite~~ considerably smooth patterns, indicating~~e~~ ~~the~~ a small change in the sea surface topography~~;~~, ~~which~~ this result is consistent with Hipkin et al. (2004). However, extreme values are observed surrounding most offshore areas, ~~such as e.g.,~~e.g. ~~–~~see the features over the offshore regions closed to The Wash (around 0.5 ℃W and 53 ℃N) and Thames estuary (around 1 ℃W and 51.5 ℃N) in England, and along the coastal areas of France, Netherlands, and Germany~~,~~. MDT signals in t~~T~~hese ~~–~~ areas are ~~which are~~traditionally difficult to model and are frequently ~~typically~~ identified as errors (Hipkin et al., 2004). The problems for computing geodetic MDTs in offshore regions are twofold. First, the quasi-geoid/geoid is poorly modeled in coastal areas due to ~~the~~ unfavorable data coverage, and data inconsistencies are usually observed when combining land and marine gravity surveys.

~~Moreover~~Further, the quality of altimetry data is dramatically reduced near ~~the~~ offshore areas, and associated errors in the derived MSS propagate into the final MDT (Andersen et al., 2013). However, airborne ~~gravity measurements~~gravimetric survey provides a seamless ~~way for~~method of gravity measurements over land and ~~seas~~oceans, which may improve this situation ~~which may allay this situation~~ (Andersen and Knudsen, 2000).

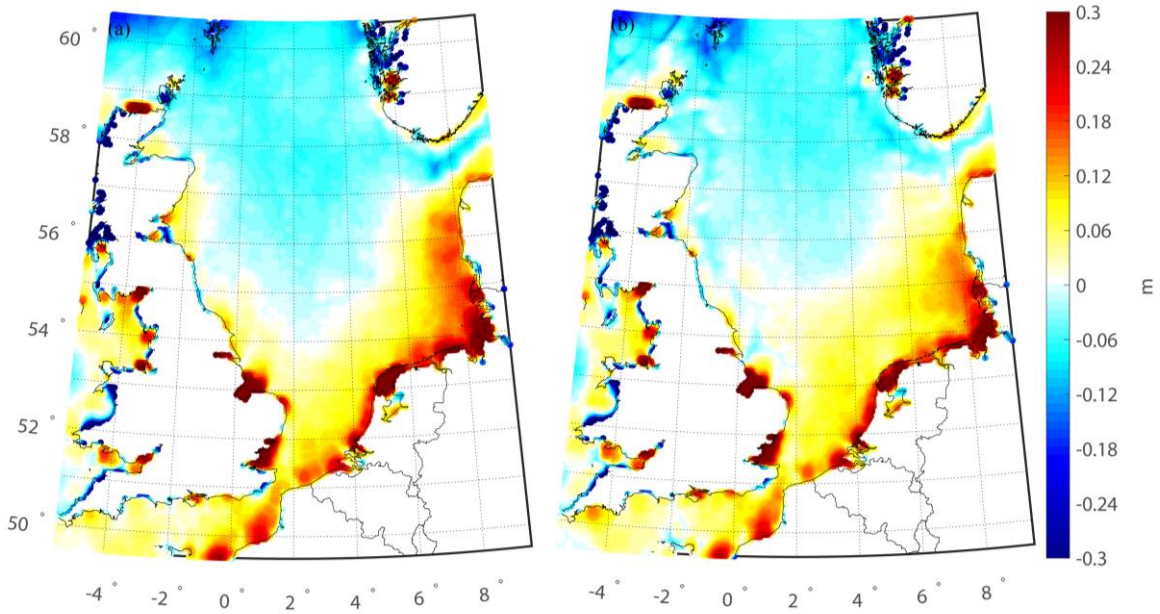

Figure 10. Different geodetic MDTs over~~in~~ the North Sea. (a) MDTNS_QGNSea; (b) MDTNS_EGG08. For all profiles, the mean values ha~~s~~ve been removed.

4. Conclusions

A multilayer approach ~~is developed~~ for gravity field recovery at the regional scale~~s~~, within the framework of multi-resolution representation, ~~was~~is developed, where the residual gravity field is parameterized as the superposition of the ~~multiply~~ multiple layers of Poisson wavelets located at ~~the~~ different depths beneath the Earth's surface~~the topography~~. Since the gravity signals ~~is~~ are the sum of the contributions ~~generated from~~of the anomaly sources at different depths, we ~~put~~ placed the ~~multiply~~ multiple layers of the model at the locations ~~where~~ of the different anomaly sources ~~situate~~. Further, wavelet decomposition and power spectrum analysis are applied ~~for~~ to ~~estimating~~ estimate the depths of the different layers.

~~For~~ To test~~ing~~ the performance of this multilayer approach, we model~~applied~~ a local gravimetric quasi-geoid model,

called QGNSea V1.0, to regions over the North Sea in Europe is modeled and compared validate thise model with otheragainst independent control data models. Based on wavelet decomposition and power spectrum analysis, multiplley layers locatedthat situate between 4.5 km and 59.2 km underneath the topography Earth's surface are builtwereare constructed to capture the signals at different scales. The numerical results show that the multilayer approach is sensitive to the spectrum of signals, both in the low- and high-frequency bands,; while, the traditionallly used single-layer approach is only sensitive for to parts of the signals' spectrum. The cComparisons with the single-layer approach show that the multilayer approach fits the gravity observations better, especially in the regions where the gravity signals show strong correlations with the variation of local topography. Moreover, we introduce an Akaike information criterion (AIC) test for different models, which is an estimator estimates of the relative quality of the statistical models for a given set of data, providing provided a means is introduced for model selection in the view of statistical test. The associated results demonstrate that the multilayer model gives obtains a smaller AIC value, which and reaches achieves a better balance between the goodness of fit of data and the simplicity of the model. The eEvaluation with using independent GPS/leveling data tests the ability of regional models recovered from different methods of towards realistic extrapolation of regional models recovered from different methods, reveals and showeds that the model called QGNSea V1.0 computed byusing the multilayer approach fits the local GPS/leveling data better than that using the single-layer approach, by the magnitudes of 0.4 cm, 0.9 cm, and 1.1 cm in the Netherlands, Belgium, and parts of Germany, respectively, compared to the one recovered from the single-layer approach. Further comparisons with the existing models show that QGNSea V1.0 has the best performanceis superior in terms of performance, which and may be beneficial for investigating the ocean circulation in the North Sea and surrounding oceanic areas.

Future work is needed forshould focus on further improving the QGNSea V1.0. First, a data-adaptive algorithm may be developed to for designing the optimal network in the multilayer approach, such as, e.g., for an algorithm for choosing the order for wavelet decomposition and determining the number of multiplley layers, since human interventions are currently needed for estimating these key parameters for the time being. Moreover, the satellite data (e.g.,e.g. K-band Range Rate data and gravity gradients) from GRACE and GOCE missions can be combined with the ground-based gravimetry and altimetry data through the multilayer approach. Doing so , which is expected tocan further improve the quality of local gravity field recovery, especially in the long-wavelength parts bands that theof satellite observations contribute. However, deeper layers than ones wethose used in this study to combine surface data

may be implemented to incorporate satellite observations, since these data mainly contribute to low-frequency bands of the gravity field. In addition, the stochastic model may need to be refined. For instance, the effects ~~on the solutions caused by~~of the GGM~~'s~~ errors on the ~~model~~ solutions ~~may~~ can be quantified if the full error variance-covariance matrix of the spherical coefficients is incorporated into the stochastic model. ~~In this way~~Thus, the different data may be more properly weighted~~,~~ and the solutions may be further improved.

Author contributions. All authors have contributed to designing the approach and writing the manuscript.

Code and data availability. The source code is included as the Supplement. Gravity data were provided by the British Geological Service; the Geological Survey of Northern Ireland; the Nordic Geodetic Commission; Bundesamt für Kartographie und Geodäsie (Germany); Institut für Erdmessung (Germany); the Bureau Gravimétrique International IAG service (France); the Banque de données Gravimétriques de la France; and the Bureau de Recherches Géologiques et Minières (France). GPS/leveling data were provided by the Geo-information and ICT of Rijkswaterstaat (RWS-AGI) and the GPS Kernnet of the Kadaster, National Geographic Institute (NGI) and the Royal Observatory (ROB), and Bundesamt für Kartographie und Geodäsie.

Competing interests. The authors declare that they have no conflict of interest.

Acknowledgments. The authors would like to give our sincerest thanks to two anonymous reviewers and Dr. Cornelis Slobbe for their beneficial suggestions and comments, which are of great value for improving and correcting the manuscript. We also thank the Executive Editor Lutz Gross for the kind assistances and constructive comments. We thank the kind supports from the editorial office. We acknowledge funding from the Netherlands Vertical Reference Frame project. Thanks Prof. Roland Klees and Dr. Cornelis Slobbe from Delft University of Technology for kindly providing the original software, and part of the work was done in Delft University of Technology under the support with the State Scholarship Fund from Chinese Scholarship Council (201306270014). This study was also supported by the National Natural Science Foundation of China (No.41830110, 41504015, 41474109), China Postdoctoral Science Foundation (No.2016M602301), the Open Research Fund Program of the State Key Laboratory of Geodesy and Earth's Dynamics (No.SKLGED2018-1-2-E and SKLGED2018-1-3-E), and Key Laboratory of Geospace Environment and Geodesy, Ministry of Education, Wuhan University (No.17-01-09).

Appendix A: Akaike information criterion

Suppose that we have a statistical model of some data, and the Akaike information criterion (AIC) value of the model

is (Burnham and Anderson, 2002)

$$AIC = 2k\text{-}2\ln(\hat{L}) \quad (1)$$

where k is the number of estimated parameters in the model, and $\hat{L}$ is the maximum value of the likelihood function for the model (Akaike, 1974; Burnham and Anderson, 2002).

For least squares fitting, the maximum likelihood estimate for the variance of a model's residuals distributions is

$$\hat{\theta}^2 = RSS / m \quad (2)$$

where RSS is the residual sum of squares (RSS), and m is the number of observations.

Then, the maximum value of a log-likelihood function of least square model is (Burnham and Anderson, 2002)

$$-\frac{m}{2}\ln(2\pi) - \frac{m}{2}\ln(\hat{\theta}^2) - \frac{1}{2\hat{\theta}^2}RSS = -\frac{m}{2}\ln(RSS / m) + C \quad (3)$$

where C is a constant independent of the model.

Combining eq. (1) and eq. (3), for least square model, the AIC value is expressed as

$$AIC = 2k + m\ln(RSS / m) + C \quad (4)$$

Since only differences in AIC are meaningful, the constant C can be ignored, and we can conveniently take $AIC = 2k + m\ln(RSS / m)$ for model comparisons.

References

Akaike, H.: A new look at the statistical model identification, IEEE Transactions on Automatic Control, 19(6), 716-723, https://doi.org/10.1109/TAC.1974.1100705, 1974.

Andersen, O. B. and Knudsen, P.: The role of satellite altimetry in gravity field modeling in coastal areas, Phys. Chem. Earth., 25(1), 17-24, https://doi.org/10.1016/S1464-1895(00)00004-1, 2000.

Andersen, O. B., Knudsen, P., and Stenseng, L.: The DTU13 global mean sea surface from 20 years of satellite altimetry, In: OSTST Meeting, Boulder, Colo, 2013.

Artemieva, I.M. and Thybo, H.: EUNAseis: A seismic model for Moho and crustal structure in Europe, Greenland, and the North Atlantic region, Tectonophysics, 609, 97-153, https://doi.org/10.1016/j.tecto.2013.08.004, 2013.

Audet, P.: Toward mapping the effective elastic thickness of planetary lithospheres from a spherical wavelet analysis of gravity and topography, Phys. Earth. Planet. In., 226(1), 48-82, https://doi.org/10.1016/j.pepi.2013.09.011, 2014.

Becker, S., Brockmann, J. M., and Schuh, W. D.: Mean dynamic topography estimates purely based on GOCE gravity

field models and altimetry, Geophys. Res. Lett., 41, 2063-2069, https://doi.org/10.1002/2014GL059510, 2014.

Bentel, K., Schmidt, M., and Rolstad, D.C.: Artifacts in regional gravity representations with spherical radial basis functions, Journal of Geodetic Science, 3(3), 173-187, https://doi.org/10.2478/jogs-2013-0029, 2013.

Bingham, R. J., Haines, K., and Lea, D. J.: How well can we measure the ocean's mean dynamic topography from space? J. Geophys. Res. Oceans, 119, 3336-3356, https://doi.org/10.1002/2013JC009354, 2014.

Blundell, D.J., Hobbs, R.W., Klemperer, S.L., Scott-Robinson, R., Long, R.E., West, T.E., and Duin, E.: Crustal structure of the central and southern North Sea from BIRPS deep seismic reflection profiling, Journal of the Geological Society, 148, 445-457, 1991.

Burnham, K. P. and Anderson, D. R.: Model Selection and Multimodel Inference: A practical information-theoretic approach (2nd ed.), Springer-Verlag, ISBN 0-387-95364-7, 2002.

Chambodut, A., Panet, I., Mandea, M., Diament, M., Holschneider, M., and Jamet, O.: Wavelet frames: an alternative to spherical harmonic representation of potential fields, Geophys. J. Int., 163(3), 875-899, https://doi.org/10.1111/j.1365-246X.2005.02754.x, 2005.

Cianciara, B. and Marcak, H.: Interpretation of gravity anomalies by means of local power spectra, Geophys. Prospect., 24 (2), 273-286, https://doi.org/10.1111/j.1365-2478.1976.tb00925.x, 1976.

Denker, H.: Regional Gravity Field Modeling: Theory and Practical Results, In: G Xu (ed)Sciences of 641 Geodesy - II, 185-291, Springer, Berlin, Heidelberg, 2013.

Eicker, A., Schall, J., and Kusche, J.: Regional gravity modeling from spaceborne data: case studies with GOCE, Geophys. J. Int., 196(3), 1431-1440, https://doi.org/10.1093/gji/ggt485, 2013.

Fengler, M.J., Freeden, W., Kohlhaas, A., Michel, V., and Peters, T.: Wavelet Modeling of Regional and Temporal Variations of the Earth’s Gravitational Potential Observed by GRACE, J. Geod., 81(1), 5-15, https://doi.org/10.1007/s00190-006-0040-1, 2007.

Fengler, M.J., Freeden, W., and Michel, V.: The Kaiserslautern multiscale geopotential model SWITCH-03 from orbit perturbations of the satellite CHAMP and its comparison to the models EGM96, UCPH2002_02_0.5, EIGEN-1s and EIGEN-2, Geophys. J. Int., 157(2), 499-514, https://doi.org/10.1111/j.1365-246X.2004.02209.x, 2004.

Fichler, C. and Hospers, J.: Deep crustal structure of the northern North Sea Viking Graben: results from deep reflection seismic and gravity data, Tectonophysics, 178, 241-254, https://doi.org/10.1016/0040-1951(90)90150-7, 1990.

Forsberg, R. and Tscherning, C.C.: An overview manual for the GRAVSOFT geodetic gravity field modeling programs,

2nd edn. National Space Institute, Denmark and Niels Bohr Institute, University of Copenhagen, 2008.

Förste, C., Bruinsma, S.L., Abrikosov, O., Lemoine, J.M., Schaller, T., Götze, H.J., Ebbing, J., Marty, J.C., Flechtner, F., Balmino, G., and Biancale, R.: EIGEN-6C4 The latest combined global gravity field model including GOCE data up to degree and order 2190 of GFZ Potsdam and GRGS Toulouse, The 5th GOCE User Workshop, Paris, France, 2014.

Fotopoulos, G.: Calibration of geoid error models via a combined adjustment of ellipsoidal, orthometric and gravimetric geoid height data, J. Geod., 79(1), 111-123, https://doi.org/10.1007/s00190-005-0449-y, 2005.

Freeden, W., Gervens, T., and Schreiner, M.: Constructive Approximation on the Sphere (With Applications to Geomathematics), Oxford Sci. Publ., Clarendon Press, Oxford, 1998.

Freeden, W., Fehlinger, T., Klug, M., Mathar, D., and Wolf, K.: Classical globally reflected gravity field determination in modern locally oriented multiscale framework, J. Geod., 83, 1171-1191, https://doi.org/10.1007/s00190-009-0335-0, 2009.

Freeden, W. and Schreiner, M.: Local multiscale modelling of geoid undulations from deflections of the vertical, J. Geod., 79, 641-651, https://doi.org/10.1007/s00190-005-0017-5, 2006.

Gilardoni, M., Reguzzoni, M., and Sampietro, D.: GECO: a global gravity model by locally combining GOCE data and EGM2008, Studia Geophysica et Geodaetica, 60 (2), 228-247, https://doi.org/10.1007/s11200-015-1114-14, 2015.

Grad, M. and Tiira, T.: The Moho depth map of the European Plate, Geophys. J. Int., 176, 279-292, https://doi.org/10.1111/j.1365-246X.2008.03919.x, 2009.

Gruber, T., Rummel, R., Abrikosov, O., and van Hees, R.: GOCE Level 2 Product Data Handbook. GO-MA-HPF-GS-0110, Issue 4.2. (http://earth.esa.int/pub/ESA_DOC/GOCE/GOMA-HPF-GS-0110_4.2-ProductDataHandbook.pdf), 2010.

Guo, J., Gao, Y., Hwang, C., and Sun, J.: A multi-subwaveform parametric retracker of the radar satellite altimetric waveform and recovery of gravity anomalies over coastal oceans, Science China Earth Sciences, 53(4), 610-616, https://doi.org/10.1007/s11430-009-0171-3, 2010.

Hipkin, R.G., Haines, K., Beggan, C., Bingley, R., Hernandez, F., Holt, J., and Baker, T.: The geoid EDIN2000 and mean sea surface topography around the British Isles, Geophys. J. Int., 157(2), 565-577, https://doi.org/10.1111/j.1365-246X.2004.01989.x, 2004.

Holschneider, M. and Iglewska-Nowak, I.: Poisson wavelets on the sphere, J. Fourier. Anal. Appl., 13(4), 405-419, https://doi.org/10.1007/s00041-006-6909-9, 2007.

Idžanović, M., Ophaug, V., and Andersen, O. B.: The coastal mean dynamic topography in Norway observed by CryoSat-2 and GOCE, Geophys. Res. Lett., 44, 5609-5617, https://doi.org/10.1002/2017GL073777, 2017.

Jiang, W., Zhang, J., Tian, T., and Wang, X.: Crustal structure of Chuan-Dian region derived from gravity data and its tectonic implications, Phys. Earth. Planet. Interiors., 212-213, 76-87, https://doi.org/10.1016/j.pepi.2012.07.001, 2012.

Klees, R. and Prutkin, I.: The combination of GNSS-levelling data and gravimetric (quasi-) geoid heights in the presence of noise, J. Geod., 84(12), 731-749, https://doi.org/10.1007/s00190-010-0406-2, 2008.

Klees, R., Tenzer, R., Prutkin, I., and Wittwer, T.: A data-driven approach to local gravity field modelling using spherical radial basis functions, J. Geod., 82(8), 457-471, https://doi.org/10.1007/s00190-007-0196-3, 2008.

Koch, K.R. and Kusche, J.: Regularization of geopotential determination from satellite data by variance components, J. Geod., 76, 259-268, https://doi.org/10.1007/s00190-002-0245-x, 2002.

Kusche, J.: A Monte-Carlo technique for weight estimation in satellite geodesy, J. Geod., 76(11), 641-652, https://doi.org/10.1007/s00190-002-0302-5, 2003.

Liang, W., Xu, X., Li, J., and Zhu, G.: The determination of an ultra-high gravity field model SGG-UGM-1 by combining EGM2008 gravity anomaly and GOCE observation data, Acta Geodaeticaet Cartographica Sinica, 47(4), 425-434, https://doi.org/10.11947/j.AGCS.2018.20170269, 2018.

Lieb, V., Schmidt, M., Dettmering, D., and Börger, K.: Combination of various observation techniques for regional modeling of the gravity field, J. Geophys. Res. Solid Earth, 121, 3825-3845, https://doi.org/10.1002/2015JB012586, 2016.

Mayer-Gürr, T., Pail, R., Gruber, T., Fecher, T., Rexer, M., Schuh, W.-D., Kusche, J., Brockmann, J.-M., Rieser, D., Zehentner, N., Kvas, A., Klinger, B., Baur, O., Höck, E., Krauss, S., and Jäggi, A.: The combined satellite gravity field model GOCO05s, Geophys Res Abs 17:EGU2015-12364, 2015.

Naeimi, M., Flury, J., and Brieden, P.: On the regularization of regional gravity field solutions in spherical radial base functions, Geophys. J. Int., 202, 1041-1053, https://doi.org/10.1093/gji/ggv210, 2015.

Nahavandchi, N. and Soltanpour, A.: Improved determination of heights using a conversion surface by combining gravimetric quasi-geoid/geoid and GNSS-levelling height differences, Stud. Geophys. Geod., 50(2), 165-180, https://doi.org/10.1007/s11200-006-0010-3, 2006.

Omang, O.C.D. and Forsberg, R.: How to handle topography in practical geoid determination: three examples, J. Geod., 74(6), 458-466, https://doi.org/10.1007/s001900000107, 2000.

Panet, I., Kuroishi, Y., and Holschneider, M.: Wavelet modelling of the gravity field by domain decomposition

methods: an example over Japan, Geophys. J. Int., 184(1), 203-219, https://doi.org/10.1111/j.1365-246X.2010.04840.x, 2011.

Pavlis, N.K., Holmes, S.A., Kenyon, S.C., and Factor, J.F.: The development and evaluation of Earth Gravitational Model (EGM2008), J. Geophys. Res., 117, B04406, https://doi.org/10.1029/2011JB008916, 2012.

Prutkin, I. and Klees, R.: On the non-uniqueness of local quasi-geoids computed from terrestrial gravity anomalies. J. Geod., 82(3), 147-156, https://doi.org/10.1007/s00190-007-0161-1, 2008.

Rummel, R., Balmino, G., Johannessen, J., Visser, P., and Woodworth, P.: Dedicated gravity field missions-Principle and aims, J. Geodyn., 33(1), 3-20, https://doi.org/10.1016/S0264-3707(01)00050-3, 2002.

Schmidt, M., Fengler, M., Mayer-Gürr, T., Eicker, A., Kusche, J., Sánchez, L., and Han, S.C.: Regional gravity modeling in terms of sphericalbase functions, J. Geod., 81(1), 17-38, https://doi.org/10.1007/s00190-006-0101-5, 2007.

Schmidt, M., Fabert, O., and Shum, C.K.: On the estimation of a multi-resolution representation of the gravity field based on spherical harmonics and wavelets, J. Geodyn., 39(1), 512-526, https://doi.org/10.1016/j.jog.2005.04.007, 2005.

Schmidt, M., Han, S.C., Kusche, J., Sanchez, L., and Shum, C.K.: Regional high- resolution spatiotemporal gravity modeling from GRACE data using spherical wavelets, Geophys. Res. Lett., 33, L08403, https://doi.org/10.1029/2005GL025509, 2006.

Sjöberg, L. E.: A discussion on the approximations made in the practical implementation of the remove-compute-restore technique in regional geoid modelling, J. Geod., 78, 645-653, https://doi.org/10.1007/s00190-004-0430-1, 2005.

Slobbe, D. C.: Roadmap to a mutually consistent set of offshore vertical reference frames, PhD thesis, The Netherland, 2013.

Slobbe, D.C., Klees, R., and Gunter, B.C.: Realization of a consistent set of vertical reference surfaces in coastal areas, J. Geod., 88(6), 601-615, https://doi.org/10.1007/s00190-014-0709-9, 2014.

Spector, A. and Grant, F.S.: Statistical models for interpreting aeromagnetic data, Geophysics, 35(2), 293-302, https://doi.org/10.1190/1.1440092, 1970.

Syberg, F.J.R.: A Fourier method for the regional-residual problem of potential fields, Geophys. Prospect., 20(1), 47-75, https://doi.org/10.1111/j.1365-2478.1972.tb00619.x, 1972.

Tapley, B. D., Bettadpur, S., Watkins, M., and Reigber, C.: The gravity recovery and climate experiment: Mission

overview and early results, Geophys. Res. Lett., 31, L09607, https://doi.org/10.1029/2004GL019920, 2004.

Tenzer, R. and Klees, R.: The choice of the spherical radial basis functions in local gravity field modeling. Stud. Geophys. Geod., 52(3), 287-304, https://doi.org/10.1007/s11200-008-0022-2, 2008.

Tenzer, R., Klees, R., and Wittwer, T.: Local Gravity Field Modelling in Rugged Terrain Using Spherical Radial Basis Functions: Case Study for the Canadian Rocky Mountains. In S. Kenyon, Geodesy for Planet Earth, International Association of Geodesy Symposia 136, Springer-Verlag Berlin Heidelberg, pp 401-409, 2012.

Tscherning, C.C.: Introduction to functional analysis with a view to its application in approximation theory. In: Moritz H, Sünkel H(eds)Approximation methods in geodesy, Karlsruhe, Germany, 1978.

Wang, J., Guo, J., Liu, X., Shen, Y., and Kong, Q.: Local oceanic vertical deflection determination with gravity data along a profile, Mar. Geod., 41(1), 24-43, https://doi.org/10.1080/01490419.2017.1380091, 2018.

Wang, Y., Saleh, J., Li, X., and Roman, D. R.: The US Gravimetric Geoid of 2009 (USGG2009): model development and evaluation, J. Geod., 86(3), 165-180, https://doi.org/10.1007/s00190-011-0506-7, 2012.

Wittwer, T.: Regional gravity field modelling with radial basis functions, Dissertation, Delft University of Technology, Delft, The Netherlands, 2009.

Wu, Y. and Luo, Z.: The approach of regional geoid refinement based on combining multi-satellite altimetry observations and heterogeneous gravity data sets, Chinese J. Geophys. (in Chinese), 59(5), 1596-1607, https://doi.org/10.6038/cjg20160505, 2016a.

Wu, Y., Luo, Z., Chen, W., and Chen, Y.: High-resolution regional gravity field recovery from Poisson wavelets using heterogeneous observational techniques, Earth Planets Space, 69:34, https://doi.org/10.1186/s40623-017-0618-2, 2017a.

Wu, Y., Luo, Z., and Zhou, B.: Regional gravity modelling based on heterogeneous data sets by using Poisson wavelets radial basis functions, Chin. J. Geophys (in Chinese), 59(3), 852-864, https://doi.org/10.6038/cjg20160308, 2016b.

Wu, Y., Zhong, B., and Luo, Z.: Investigation of the Tikhonov regularization method in regional gravity field modeling by Poisson wavelets radial basis functions, Journal of Earth Science, 9, 1-10, https://doi.org/10.1007/s12583-017-0771-32016, 2017b.

Wu, Y., Zhou, H., Zhong, B., and Luo, Z.: Regional gravity field recovery using the GOCE gravity gradient tensor and heterogeneous gravimetry and altimetry data, J. Geophys. Res. Solid Earth, 122(8), 6928-6952, https://doi.org/10.1002/2017JB014196, 2017c.

Xu, C., Liu, Z., Luo, Z., Wu, Y., and Wang, H.: Moho topography of the Tibetan Plateau using multi-scale gravity

analysis and its tectonic implications, J. Asian. Earth. Sci., 138, 378-386, https://doi.org/10.1016/j.jseaes.2017.02.028, 2017.

Xu, C., Luo, Z., Sun, R., Zhou, H., and Wu, Y.: Multilayer densities using a wavelet-based gravity method and their tectonic implications beneath the Tibetan Plateau, Geophys. J. Int., 213, 2085-2095, https://doi.org/10.1093/gji/ggy110, 2018.

Ziegler, P.A. and Dèzes, P.: Crustal evolution of western and central Europe, European Lithosphere Dynamics, In: Gee, D., Stephenson, R. (Eds.), Geol. Soc. London Sp. Publ., 32, 43-56, 2006.